

**GENESIS OF HIGH-SULFIDATION VINCIENNITE-BEARING Cu–As–Sn (\pm Au)
ASSEMBLAGE FROM THE RADKA EPITHERMAL COPPER DEPOSIT,
BULGARIA: EVIDENCE FROM MINERALOGY
AND INFRARED MICROTHERMOMETRY OF ENARGITE**

KALIN KOUZMANOV[§] AND CLAIRE RAMBOZ

Institut des Sciences de la Terre d'Orléans (ISTO–CNRS), 1A, rue de la Férollerie, F–45071 Orléans Cedex 2, France

LAURENT BAILLY

BRGM, REM/MESY, B.P. 6009, F–45060 Orléans Cedex 2, France

KAMEN BOGDANOV

*Department of Mineralogy, Petrology and Economic Geology, Faculty of Geology and Geography,
Sofia University “St. Kliment Ohridski”, 15 Tsar Osvoboditel Boulevard, 1000 Sofia, Bulgaria*

ABSTRACT

The Radka deposit is one of the largest Cu–Au epithermal deposits related to Late Cretaceous volcanic arc-type magmatic activity in the Panagyurishte ore region, central part of the Srednogorie zone, Bulgaria. The mineralogical and geochemical features of a vinciennite-bearing Cu–As–Sn (\pm Au) assemblage at Radka show very similar characteristics to those in other vinciennite-bearing high-sulfidation epithermal deposits worldwide. The assemblage consists of enargite, Cu-excess tennantite, chalcopyrite, gold, vinciennite, colusite, and minor covellite, within a gangue of barite, illite, and quartz. A detailed electron-microprobe study of vinciennite and associated minerals reveals the heterovalency of Cu and Fe. New data on the composition of vinciennite sheds light on aspects of its crystal chemistry, such as incorporation of Cu²⁺ and Fe³⁺ and Sn⁴⁺ \rightleftharpoons Ge⁴⁺ substitution, and leads us to propose a new empirical formula: Cu₈Cu²⁺₂Fe³⁺₃(Fe,Cu)²⁺(Sn,Ge)⁴⁺(As,Sb)⁵⁺S₁₆²⁻. Infrared microthermometry of enargite-hosted fluid inclusions provides constraints on the conditions of deposition of this unusual assemblage in the context of the evolution of the magma-related ore-forming system at Radka. The assemblage was formed by oxidized and slightly acid fluids, with a dominantly magmatic signature, high fugacity of sulfur and intermediate salinity (about 10 wt.% eq. NaCl) at a temperature of about 275°C. In view of the geology of the Radka deposit, its mineralogical and geochemical peculiarities, ore textures, type of hydrothermal alteration and the character of the fluids, we interpret the deposit as a deep part of a high-sulfidation epithermal mineralization, possibly genetically related to a porphyry copper system.

Keywords: vinciennite, enargite, mineralogy, infrared microthermometry, fluid inclusions, epithermal, Srednogorie, Radka, Bulgaria.

SOMMAIRE

Radka est un des plus gros gisements épithermaux de cuivre et or de la région minière de Panagyurishte, dans la partie centrale de la zone de Srednogorie, en Bulgarie. Le développement de ce district métallogénique est lié à une activité magmatique néocrétacée de type arc insulaire. Les particularités minéralogiques et géochimiques de la paragenèse Cu–As–Sn (\pm Au) à vinciennite sont très semblables à celles décrites dans d'autres gisements de type épithermal acide. La paragenèse contient énérgite, tennantite riche en cuivre, chalcopyrite, or, vinciennite, colusite et covellite en trace, dans une gangue de barite, illite et quartz. L'étude de la vinciennite et des phases associées à la microsonde électronique révèle que le cuivre et le fer dans ces minéraux sont hétérovalents. Les nouvelles données obtenues sur la composition de la vinciennite nous ont permis d'élucider certains aspects de sa cristallogénèse, tels que l'incorporation de Cu²⁺ et Fe³⁺ et la substitution Sn⁴⁺ \rightleftharpoons Ge⁴⁺, et de proposer une nouvelle formule structurale: Cu₈Cu²⁺₂Fe³⁺₃(Fe,Cu)²⁺(Sn,Ge)⁴⁺(As,Sb)⁵⁺S₁₆²⁻. L'étude microthermométrique des inclusions fluides dans l'énérgite au microscope infrarouge a permis de déterminer les conditions de formation de cette paragenèse inhabituelle dans le contexte de l'évolution du système magmato-hydrothermal de Radka. La minéralisation a été formée par des fluides relativement oxydés et

[§] *Present address:* Institute of Isotope Geochemistry and Mineral Resources, ETH Zentrum, NO F52.1, Sonneggstrasse 5, CH-8092 Zürich, Switzerland. *E-mail address:* kouzmanov@erdw.ethz.ch

légèrement acides, avec une composante magmatique dominante, une fugacité du soufre élevée et une salinité intermédiaire (environ 10% poids équiv. NaCl) à une température de l'ordre de 275°C. Les particularités géologiques du gisement de Radka, sa composition minéralogique et géochimique, ainsi que les textures du minerai, le type d'altération hydrothermale et le caractère des fluides, nous ont permis de définir le gisement comme une partie profonde d'un système épithermal acide, tout en envisageant une relation génétique avec un système de type porphyre cuprifère en profondeur.

Mots-clés: vinciennite, énergite, minéralogie, microthermométrie infrarouge, inclusions fluides, épithermal, Srednogorie, Radka, Bulgarie.

INTRODUCTION

The Radka deposit is one of the largest Cu–Au epithermal deposits in the Panagyurishte ore district, Bulgaria. The district is part of the Srednogorie zone (Fig. 1), which is the Bulgarian portion of the most im-

portant ore-bearing igneous belt of calc-alkaline signature within the Alpine – Balkan – Carpathian – Dinaride realm, defined as Banatic Magmatic and Metallogenic Belt, BMMB (Berza *et al.* 1998, Ciobanu *et al.* 2002) or Banat–Srednogorie Tectonic and Metallogenic Zone, BSTMZ (Popov 1996). The Late Cretaceous in-

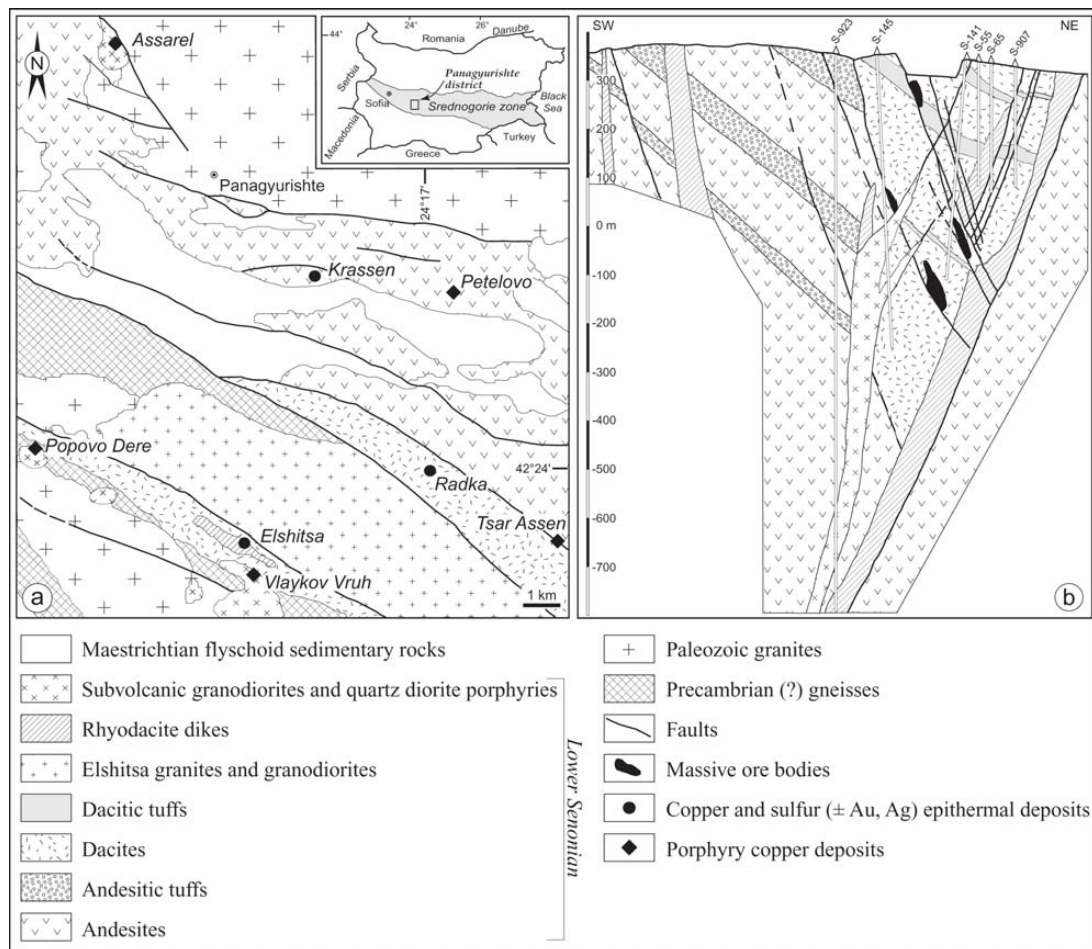


FIG. 1. a) Position of the Srednogorie zone and geology of the southern part of the Panagyurishte district with location of the major mineral occurrences (modified from Bogdanov 1980). b) Cross-section of the Radka deposit (after Popov & Popov 1997, Tsonev *et al.* 2000b).

trusive and volcanic rocks of the belt, including minor tholeiitic and alkaline, but mostly calc-alkaline, high-K calc-alkaline to shoshonitic compositions (Stanisheva-Vassileva 1980, Berza *et al.* 1998) host two major styles of ore deposits: porphyry copper, and “replacement massive sulfide epigenetic” (Jankovic 1977, Bogdanov 1980) or high sulfidation epithermal deposits (according to the modern classification: White & Hedenquist 1990, Sillitoe 1999). The existence of these deposits is one of the unusual features of the BSTMZ because (a) the two types of mineralization are not only intimately spatially but also genetically related (Popov & Popov 1997, Strashimirov *et al.* 2002), and (b) the epithermal deposits show extremely varied and, in some cases, unusual mineralogical and geochemical features (Petrunov 1994, Tsonev *et al.* 2000b, Kouzmanov 2001).

In this paper, we provide detailed information about the mineralogical and geochemical features of a vincienite-bearing Cu–As–Sn (\pm Au) assemblage from the Radka deposit, Bulgaria. The mineral chemistry of vincienite and related minerals coupled with an infrared (IR) microthermometric study of enargite-hosted fluid inclusions allow us to constrain the conditions of deposition of this unusual assemblage in the context of the evolution of the magma-related ore-forming system at Radka.

GEOLOGICAL SETTING

The Radka deposit is located in the southeastern part of the Panagyurishte district, situated in the central part of the Srednogie zone (Fig. 1a). The district is economically the most significant copper province in Bulgaria (more than 95% of the Bulgarian copper and gold production), with more than 10 deposits and numerous occurrences of ore.

The Panagyurishte district is located at the intersection of longitudinal subequatorial and diagonal N–NW-trending faults and has characteristics of a magmato-tectonic corridor with a rough northwesterly direction, which covers an area of about 1500 km². The geology consists of Precambrian (?) gneisses and Paleozoic granites overprinted by a Late Cretaceous volcano-plutonic complex (Fig. 1a). In some parts of the district, these rocks are covered by Maestrichtian flyschoid sedimentary rocks and small outcrops of Paleogene and Neogene molasse (Bogdanov 1980). Late Cretaceous magmatic activity, dated at 92.3 ± 1.4 Ma in the northern part of the district to 82.25 ± 0.4 Ma in the southern part (U–Pb method on zircon; Von Quadt *et al.* 2001) and involving magmas calc-alkaline to subalkaline in composition, is closely related to the two main types of ore deposits: massive epigenetic Cu–S \pm Ag–Au deposits of replacement origin (Krassen, Radka and Elshitsa) and porphyry copper deposits (Assarel, Petelovo, Tsar Assen, Vlaykov Vruh and Popovo Dere (Fig. 1a; Bogdanov 1980, Popov & Popov 1997). Re-

cently, Tsonev *et al.* (2000a) defined the Radka deposit as a transitional epithermal system with an intermediate sulfidation style of mineralization, closer to the high sulfidation type, in agreement with the original epigenetic theory of Dimitrov (1960) and consistent with current genetic models of ore formation in the porphyry–epithermal environment (Hedenquist & Lowenstern 1994, Hedenquist & Arribas 1999, Hedenquist *et al.* 2000). Recent radiogenic and stable isotope data from the southern part of the Panagyurishte district confirm that both metals and sulfur in the ore deposits are of magmatic origin (Kouzmanov 2001).

The official production from the Radka deposit over the interval 1942–1995 was 6.39 million t of copper ore grading 1.06% Cu, and 0.28 million t of pyrite ore grading 28.6% S, with a total production of 68,006 t of copper and 78,954 t of sulfur (Milev *et al.* 1996). Gold and silver were extracted as a by-product from the pyrite and copper concentrate. The mine closed in 1995. The deposit consists of several steeply dipping, lenticular massive orebodies with a halo of veinlets and disseminated mineralization. Ore is confined to fault zones striking west–northwest and is hosted by felsic volcanic rocks (dacite lavas, tuffs and tuff breccias), cross-cut by rhyodacite dikes (Fig. 1b; Dimitrov 1960).

TYPES OF ORE, PARAGENETIC RELATIONSHIPS, HYDROTHERMAL ALTERATION AND FLUIDS AT RADKA

Two main types of ore exist at Radka. Massive ores, with as much as 85–90% of sulfides, form lenticular or stock-like bodies, locally with highly variable morphology. The complex history of hypogene mineralization at Radka has been grouped into nine ore-forming stages. The mineralogical succession is summarized in Figure 2. The main minerals in the massive ores are pyrite, chalcopyrite, bornite, tennantite, enargite, sphalerite, galena and chalcocite. Numerous subordinate and rare Ge-, Ga-, In-, Sn-, Bi- and Te-bearing minerals also are present (Tzonev 1982, Kovalenker *et al.* 1986, Kouzmanov *et al.* 2000b; Fig. 2). Owing to their high permeability, dacitic volcanic breccia and tuffs form the most favorable environment for metasomatic replacement and hydrothermal precipitation (Fig. 3a). Wallrock alteration is structurally and morphologically related to ore-controlling faults. Radonova (1962) and Chipchakova *et al.* (1981) described the zonation of alteration from the orebodies outward consisting of quartz – white mica, quartz – chlorite – white mica and propylitic assemblages. The second type of ore occurs as veins, veinlets or dissemination of pyrite, chalcopyrite and quartz at the periphery of massive bodies.

A particular feature of the Radka deposit is the presence of clasts of massive fine-grained to colloform pyrite in a polymictic breccia affected by quartz – white mica alteration (Fig. 3b; Bogdanov *et al.* 1970). The pyrite from these clasts corresponds to the massive pyrite formed during the first stage of Fe (\pm As, Cu) min-

eralization (Fig. 2). Breccia occurs as dikes cross-cutting the massive dacite (Fig. 3c). Breccia clasts have a polymictic composition (dacite, dacitic tuffs, massive pyrite), are subrounded to rounded, and rarely are angular in shape. Silt- and sand-sized clastic grains, extremely altered to quartz – white mica ± argillic minerals, constitute the breccia matrix. The same texture was observed under the microscope, affecting the massive orebodies (Fig. 3d). These macro- and microbreccia dikes indicate a process of fluidization of rock and ore fragments in upward-escaping fluid channelways that took place after the deposition of the first mineralized assemblage (Fig. 2). The fluidized breccias, together with the observed intense fracturing, *in situ* brecciation, and pebble-dike-like textures (Kouzmanov 2001), are very common characteristics of many hydrothermal systems formed in a porphyry to epithermal transitional environment (Sillitoe 1985, Corbett & Leach 1998).

Limited fluid-inclusion data for the Radka deposit are available in Strashimirov & Kovachev (1992). They reported a homogenization temperature (T_h) of 225°–245°C for inclusions in quartz from the early Fe (± As, Cu) assemblage, and T_h between 180° and 230°C in anhydrite [late Ca (± Fe) assemblage]. We performed an extensive study of quartz-hosted, primary fluid inclusions from the main Cu (± Bi, Te, Pb, As) stage (Kouzmanov *et al.* 2000a), and succeeded in identifying by micro-Raman spectrometry trapped kaolinite and white mica in these inclusions and CO₂, H₂ ± N₂ in the volatile phase. Microthermometric measurements indicate salinities ranging from 2.4 to 3.4 wt.% eq. NaCl with a mean of 2.8 ± 0.3 wt.% eq. NaCl. The inclusions homogenize to the liquid between 218 and 260°C, with a mode at 250°C. The presence of kaolinite and illite as trapped minerals in these primary fluid inclusions indicates that they contain a mildly acidic fluid with a pH of about 4 at 250°C (Heald *et al.* 1987). The slight acidity

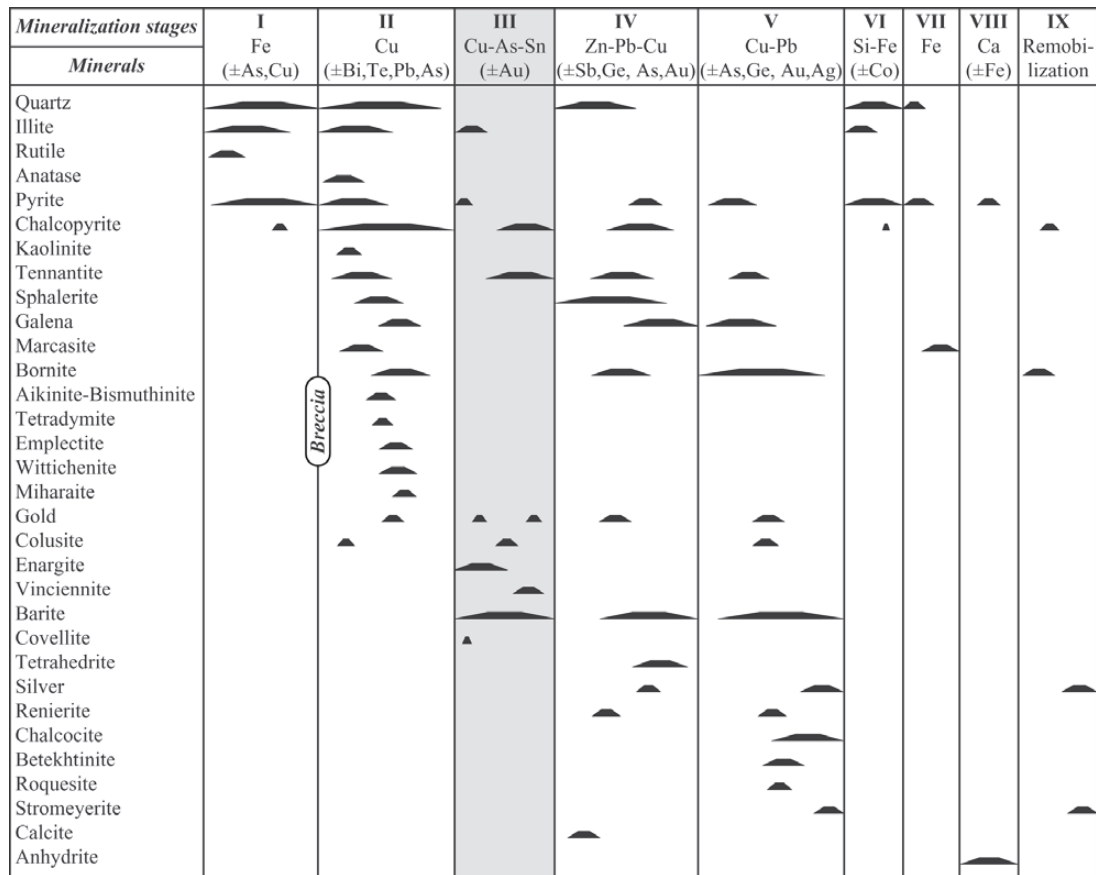


FIG. 2. Position of the Cu–As–Sn (± Au) assemblage within the mineralogical succession of the Radka ore deposit.

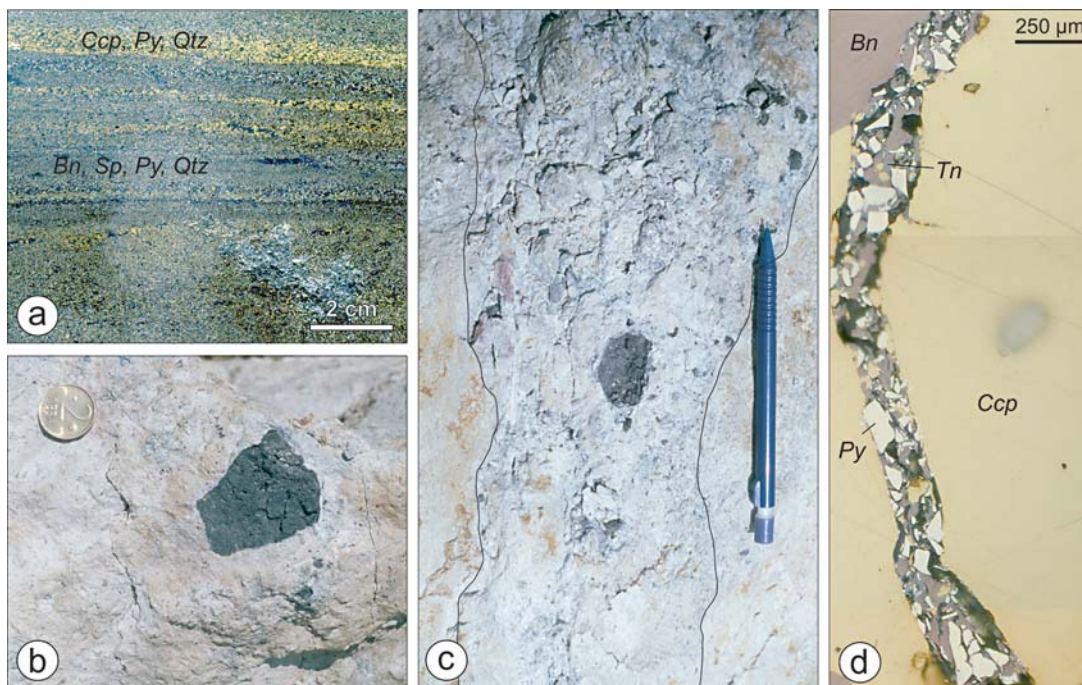


FIG. 3. Ore textures from the Radka deposit. a) Selective replacement of dacitic tuffs by pyrite (Py), chalcopyrite (Ccp), bornite (Bn), sphalerite (Sp) and quartz (Qtz). b) Subrounded clast of massive fine-grained pyrite from the first stage of mineralization in fluidized breccia affected by intensive "quartz-sericite" alteration. Scale 2.5 cm. c) Fluidized breccia dike with subrounded to rounded clasts of massive pyrite, dacitic tuffs and dacite, cross-cutting massive dacite. Both the breccia and the host rock are affected by "quartz-sericite" alteration. d) "Micro breccia dike" structure with pyrite clasts cross-cutting the massive orebodies. Breccia matrix and host environment are replaced by later chalcopyrite, bornite and tennantite (Tn). Microphotograph in reflected light.

of the fluids during this stage is also confirmed by deposition of marcasite, which precipitates only at a pH less than 5 (Murowchick & Barnes 1986). Infrared microthermometry of pyrite-hosted fluid inclusions from the Si-Fe (\pm Co) stage in Radka suggests a late reheating of the system (T_h up to 365°C) by low bulk-salinity fluids (3.5–4.6 wt.% eq. NaCl), interpreted as a magmatic vapor condensate (Kouzmanov *et al.* 2002). Sulfur isotopic data ($\delta^{34}\text{S} \approx 0\text{‰}$) for this generation of pyrite support this interpretation (Kouzmanov 2001).

ANALYTICAL TECHNIQUES

Electron-microprobe analyses (EMPA) were performed with a CAMECA SX 50 electron microprobe (BRGM – CNRS – Université d'Orléans laboratory) operated at an acceleration potential of 20 kV, a probe current of 40 nA and with a beam diameter of 1 μm . Counting times were 10 s. We used $K\alpha$ lines for Fe, Cu, S, Zn, and V, $L\alpha$ lines for As, Sb, Ag, Se, Te, Au, Sn, and Ge, and the $M\alpha$ line for Bi. For standards, we used

pure metals for Cu, Ag, Se, Au, Bi, Te, Ge, and V, pyrite for Fe, S, stibnite for Sb, sphalerite for Zn, cassiterite for Sn, and synthetic GaAs for As. Apparent concentrations were corrected for matrix effects with the PAP correction program (Pouchou & Pichoir 1984).

Selected samples, after reflected light microscopy, were examined using a JEOL JSM 6400 scanning electron microscope (SEM) equipped with a KEVEX Delta energy-dispersion spectrometer (EDS) at the Ecole Supérieure de l'Énergie et des Matériaux (Université d'Orléans).

Doubly polished sections (140–180 μm in thickness) were used for a fluid-inclusion study in enargite and quartz at the Infrared Microthermometry Laboratory of the BRGM in Orléans using a USGS gas-flow heating-freezing system mounted on an Olympus BHSM-IR microscope equipped with an infrared TV camera that allows IR observations up to 2,500 nm (Lüders 1996). Synflin standards and natural inclusions in fluorite were measured for calibration using the IR equipment and also in normal transmitted light.

RESULTS: MINERALOGY
OF THE CU-AS-SN (\pm AU) ASSEMBLAGE

The Cu-As-Sn (\pm Au) assemblage formed during the third stage of mineralization at Radka (Fig. 2), occurs as pervasive replacement and in thin veins cross-cutting the massive pyrite \pm chalcopyrite ore deposited during the first two stages (Fig. 4a). The mineral assemblage consists of enargite, tennantite, chalcopyrite, gold, vincienite, colusite, and minor covellite, within a gangue of barite, illite and very fine-grained silica.

Enargite, Cu_3AsS_4 , is the dominant sulfide mineral precipitating at the beginning of this stage. It forms polycrystalline masses filling fractures and intergranular voids within pyrite and chalcopyrite from the previous stages (Fig. 4b). The low-temperature polymorph of Cu_3AsS_4 , luzonite, has not been observed in Radka. The composition of enargite is close to being stoichiometric. Its most significant feature is the presence of small amounts of Sb (0.09–1.52 wt.%). Growth zoning in enargite, observed on BSE images (Figs. 5a, f), and IR transmitted-light microphotographs (Figs. 6b, d), is due to the substitution of Sb for As. Other trace elements detected by EMPA are minor Fe (300–5,800 ppm) and Ag (800–1,800 ppm). The content of tin and zinc is below the detection limit, 400 and 700 ppm, respectively. Locally intergrown with the enargite is illite, whose composition has a phengitic character. Enargite is partly replaced by a more abundant paragenesis with dominant tennantite, chalcopyrite and vincienite.

Tennantite is the most common mineral in the assemblage studied. It is intimately associated with chalcopyrite. Tennantite–chalcopyrite aggregates were observed as a replacement of enargite (Fig. 4c) as well as forming a symplectitic intergrowth (Fig. 5e). The tennantite is exceptionally rich in Cu [an average of 11 atoms per formula unit (*apfu*) Cu for a total of 12 metal atoms; Table 1]. According to Marcoux *et al.* (1994), it can be characterized as “Cu-excess” tennantite. Minor

Ag (up to 0.71 wt.%) and Bi (up to 0.51 wt.%) were also recorded. The mineral is poor in Zn, Sn, Te and Se (Table 1). The tennantite is completely opaque in IR transmitted light. This opacity could be due to the high Fe content (as much as 4.30 wt.%, corresponding to 1.13 *apfu*; Table 1), which is consistent with the interpretation of Campbell *et al.* (1984) that one atom of Fe per formula unit is the effective upper limit for IR transparency of tennantite. Hall *et al.* (1974) obtained similar results on synthetic samples of tetrahedrite, where only the Zn_2 tetrahedrite end-member was transmitting in the red and near infrared. Comparable observations have been made by Charlat & Lévy (1974) on Fe-poor (<1 wt.%) tetrahedrite. Recently, Lüders (1999) provided new data showing that the As-rich end-member of the tetrahedrite–tennantite solid-solution series is usually opaque in IR transmitted light, which limits the application of this technique to studies of fluid inclusions in the Sb end-member only (*i.e.*, tetrahedrite).

Chalcopyrite is intergrown with tennantite or fills intergranular voids within enargite. In some samples, a secondary bornite – chalcocite – covellite assemblage almost completely replaced the chalcopyrite (Figs. 4d, 5a, c). The only trace element in chalcopyrite detected by EMPA is As (500–5500 ppm). The composition of chalcopyrite is nearly stoichiometric, with a slight excess of Cu (Cu:Fe atomic ratio in the range from 1.04 to 1.17).

Gold is a common mineral in this assemblage. It precipitated at two intervals during the third mineralizing stage (Fig. 2). The gold, which appears as inclusions in enargite (Fig. 4d), is richer in Ag (11.8–12.8 wt.%) than the gold coprecipitated with tennantite (7.4–7.8 wt.% Ag). Both generations contain minor Cu (0.25–0.98 wt.%), without any other trace element detectable by EPMA.

Lamellar crystals of *covellite* (length:width ratio in the range 20–30) are fairly uncommon at Radka. They occur as inclusions in barite (Fig. 5d) and in some re-

TABLE 1. REPRESENTATIVE COMPOSITIONS OF CU-EXCESS TENNANTITE FROM THE RADKA DEPOSIT, BULGARIA

	1	2	3	4	5	6	7	8	9	10	11	Ave.	Emp.
Cu wt.%	48.46	48.48	47.35	47.53	47.34	47.80	47.53	46.10	46.26	46.64	47.00	47.32	11.00
Ag	0.11	0.09		0.20	0.50	0.23	0.71					0.17	0.02
Fe	3.30	3.00	3.96	3.84	3.68	3.44	3.64	3.91	3.80	3.72	4.30	3.69	0.98
As	19.46	19.44	19.50	18.70	18.78	18.60	18.97	19.81	19.17	19.69	19.56	19.24	3.79
Sb	0.37	0.41	2.16	2.77	3.34	3.27	2.72	0.82	0.81	0.89	0.84	1.67	0.20
Bi	0.51	0.53							0.15			0.11	0.01
S	28.48	28.05	28.57	28.29	28.39	28.08	28.20	28.94	28.30	28.26	28.48	28.37	13.07
Total	100.69	100.00	101.54	101.33	102.03	101.42	101.77	99.58	98.49	99.20	100.18	100.57	

The levels of Zn, Sn, Te and Se are systematically below the detection limit of the electron microprobe: 0.09, 0.05, 0.09 and 0.05 wt.%, respectively. The empirical formula, EMP, was calculated on the basis of $\Sigma Me = 12$ atoms applied to the average composition (Ave.) shown in the previous column.

crystallized pyrite at the periphery of enargite–tennantite veins. On the basis of textural relationships, we assume that enargite and covellite precipitated almost contemporaneously at the beginning of stage III of mineralization.

Tzonev (1982) described for the first time in Radka an “orange-brown sulfide” with a composition $\text{Cu}_{5.08}\text{Fe}_{1.95}\text{Sn}_{0.50}\text{As}_{0.47}\text{Sb}_{0.07}\text{S}_{7.99}$. Three years later, Cesbron *et al.* (1985) defined vinciennite as a new mineral species, with an empirical formula $\text{Cu}_{10}\text{Fe}_4\text{Sn}(\text{As},\text{Sb})\text{S}_{16}$, based on their study of samples from the Chizeuil and Huaron deposits (France and Peru, respectively). Kovalenker *et al.* (1986) confirmed the presence of vinciennite at Radka. *Vinciennite* is the main tin-bearing mineral at Radka and occurs within the paragenesis replacing enargite. It appears as amoeboid inclusions in chalcopyrite (Fig. 5b) and generally forms euhedral crystals on the margin of patches of enargite (Figs. 4d, 5c). Vinciennite grains reach 400 μm in size. They appear to be zoned on BSE images (Fig. 5a). An extensive EMPA study of vinciennite (Table 2) reveals the presence of Sb (0.36–1.23 wt.%) and Ge (0.19–1.32 wt.%). All the analyses show slight cationic excess relative to the ideal stoichiometric composition, with an average $\Sigma\text{cations}:\text{S}$ ratio of 1.06 (Table 2). In near-IR transmitted light, vinciennite is opaque.

Colusite appears associated with vinciennite (Fig. 5c) or occurs as isolated inclusions in enargite (Fig. 5f). Distinct zoning, in some cases observable even in reflected polarized light, is a very common feature of colusite from Radka. BSE images reveal a mosaic structure in the central part of the crystals (Fig. 5f). Almost all microprobe analyses of colusite (Table 3) display the constant presence of Fe (0.44–1.94 wt.%), Sb (1.22–3.92 wt.%) and Ge (0.22–1.14 wt.%).

MICROTHERMOMETRIC STUDY

IR microthermometry of enargite

Both primary and secondary fluid inclusions have been observed in enargite using the transmitted-light IR microscope (Fig. 6). Both types are two-phase and liquid-rich. *Primary inclusions* appear as isolated inclusions parallel to growth zones (Figs. 6b, d) or are attached to different solids trapped during the crystal growth of enargite (Figs. 6a, c). The latter feature is commonly interpreted as a criterion for the primary origin of fluid inclusions (Roedder 1984), *e.g.*, fluid inclusions attached to chalcopyrite crystals trapped in sphalerite (Sawkins 1964). These fluid inclusions, formed in the “shadow” of trapped solids, are generally elongate, with their long axis parallel to the direction of crystal growth (Fig. 6a). Most primary inclusions in enargite are flat, tabular to isometric, rarely with striated faces (Fig. 6b). They are small, with a diameter rarely exceeding 15 μm . *Secondary inclusions* decorate

healed fractures cross-cutting growth zones in enargite (Fig. 6e). They are isometric and small (<10 μm), regularly distributed along the fracture. Their degree of filling (0.85–0.90) is similar to that of primary inclusions and almost constant from one inclusion of the fracture to another.

No change in the IR-transparency of enargite was observed during heating runs. Freezing runs were performed before heating. Melting and homogenization temperatures, measured using the cycling technique (Goldstein & Reynolds 1994), are reproducible within analytical error. Microthermometric results for enargite-hosted fluid inclusions are summarized in Table 4. Homogenization temperatures for primary inclusions are within the restricted range of 235°–252°C; only one inclusion homogenized at 304°C. Secondary inclusions yield slightly lower values of T_h . It was not possible to determine the first melting point of ice, either in primary or in secondary inclusions. Clathrate formation was not observed upon cooling. Final melting temperatures of ice ($T_{m\text{ ice}}$), interpreted after Bodnar (1993), indicate salinities of 9.7–10.2 wt.% eq. NaCl for primary inclusions. The salinities of two secondary inclusions fall in the same range. The small size of secondary inclusions limited their suitability for microthermometric measurements.

Fluid inclusions in quartz phenocrysts

To complete the existing data on fluid inclusions at Radka, some microthermometric measurements were performed on trails of secondary fluid inclusion in quartz phenocrysts from the wallrock (mainly dacitic volcanic rocks). Two types of inclusions can be distinguished. The dominant type includes liquid-rich, two-phase fluid inclusions, with a vapor filling of 30–35% by volume (Fig. 7a). The second type consists of halite-saturated inclusions, liquid–vapor–NaCl-filled at room temperature (Fig. 7b), with highly variable volume-proportions of the three phases. The second type of inclusion is much less abundant than the first. All fluid inclusions in magmatic quartz appear secondary, and the time relationships between these two types of inclusion are unclear.

Results of microthermometric measurements on quartz-phenocryst-hosted fluid inclusions are presented in Table 4. The two-phase inclusions homogenize into liquid in the temperature range between 296°C and 323°C and have a low salinity (2.7–4.6 wt.% eq. NaCl), determined from the $T_{m\text{ ice}}$ using the equation of Bodnar (1993). Final homogenization of the three-phase fluid inclusions is taken as the higher of either the disappearance of the vapor bubble ($T_{h\text{ L-V}}$), or the dissolution of halite ($T_{m\text{ NaCl}}$). The majority of the inclusions homogenize by halite dissolution (Fig. 8). The salinities of these inclusions were determined from the dissolution temperatures of halite (Sterner *et al.* 1988) and are within the range of 31.2 to 46.0 wt.% eq. NaCl.

DISCUSSION

Mineral chemistry of vinciennite and associated minerals

Radka is one of the few ore deposits in the world where vinciennite has been described; others include the Chizeuil massive pyrite deposit, France, the Huaron epithermal polymetallic deposit, Peru (Cesbron *et al.* 1985), the Maggie porphyry copper–molybdenum deposit, British Columbia (Jambor & Owens 1987), the Layo epithermal deposit, southern Peru (Marcoux *et al.* 1994), and the Kidd Creek volcanogenic massive sulfide deposit, western Abitibi Subprovince, Canada (Hannington *et al.* 1999). Kovalenker (1982) described a “stannoidite-like” mineral with a composition corresponding to vinciennite in a subvolcanic gold deposit from the central Tien-Shan range in the former Soviet Union.

In most of these deposits, the vinciennite-bearing assemblage has very similar mineralogical and geochemical (Cu–As–Sn) features. One of these features is the presence of “Cu-excess” tennantite as one of the most abundant minerals in the paragenesis. As a rule, in all deposits the tennantite is depleted in Zn and has more than 10 *apfu* Cu for a total of 12 metal atoms. Given that the formula for the ideal end-member tennantite is $\text{Cu}_{10}(\text{Fe}, \text{Zn})_2\text{As}_4\text{S}_{13}$, the excess of Cu substituting for $(\text{Fe}, \text{Zn})^{2+}$ either indicates the presence of Cu^{2+} , or of Cu^+ in excess if the sum of metal atoms is over 12 for $4[\text{As} + \text{Sb}]$ (Charnock *et al.* 1989, Marcoux *et al.* 1994). The importance of this variety of tennantite as an indicator for the oxidation state of Fe during the ore formation was pointed out by Marcoux *et al.* (1994) and illustrated by them using the $\text{Cu}^*-\text{Fe}-(\text{Zn} + \text{Hg})$ diagram of Charlat & Lévy (1974). Compositions of “Cu-excess tennantite” from Radka compared to other vinciennite-bearing deposits are reported on the same

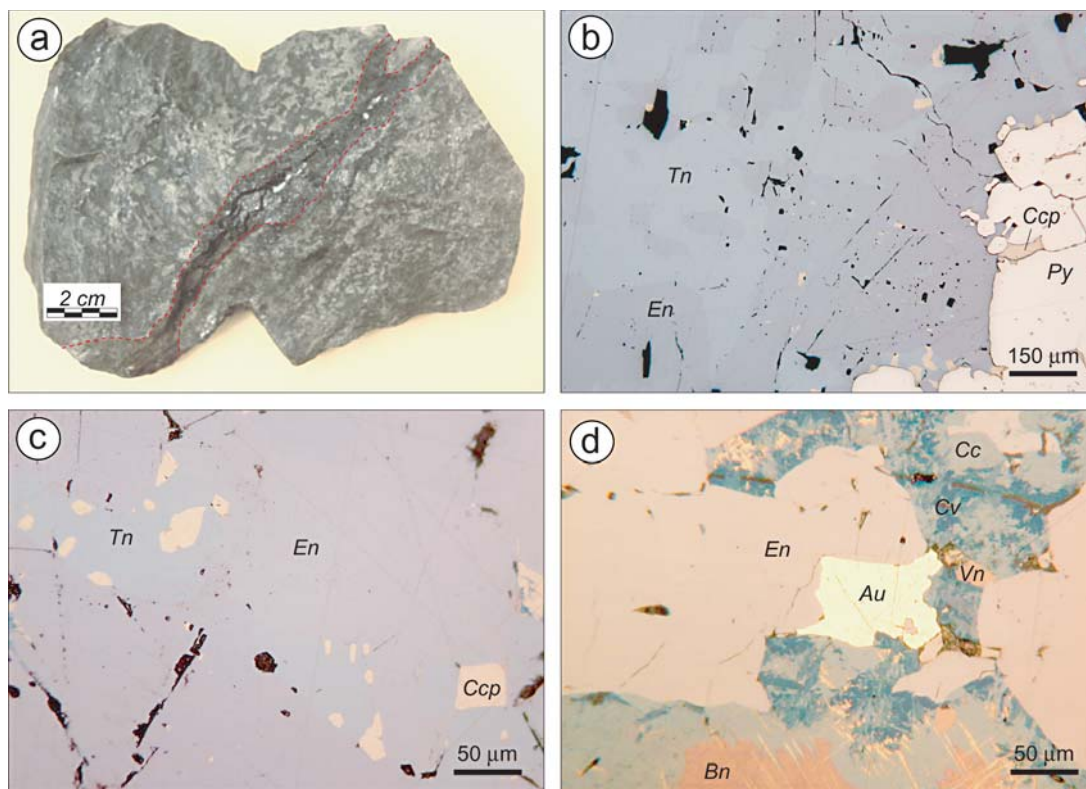


FIG. 4. Stage-III mineral assemblage. a) Tennantite – enargite ± barite vein cross-cutting massive pyrite ± chalcopyrite ore. The red dotted line marks the vein margins. b) Tennantite (Tn) – enargite (En) association replacing massive pyrite (Py) with minor chalcopyrite (Ccp) from the second stage of mineralization. c) Tennantite and chalcopyrite replacing enargite. d) Gold (Au) associated with enargite and minor vinciennite (Vn). Secondary bornite (Bn) – chalcocite (Cc) – covellite (Cv) assemblage replaces the chalcopyrite in interstices. Figures 4b, c and d are microphotographs taken in reflected light.

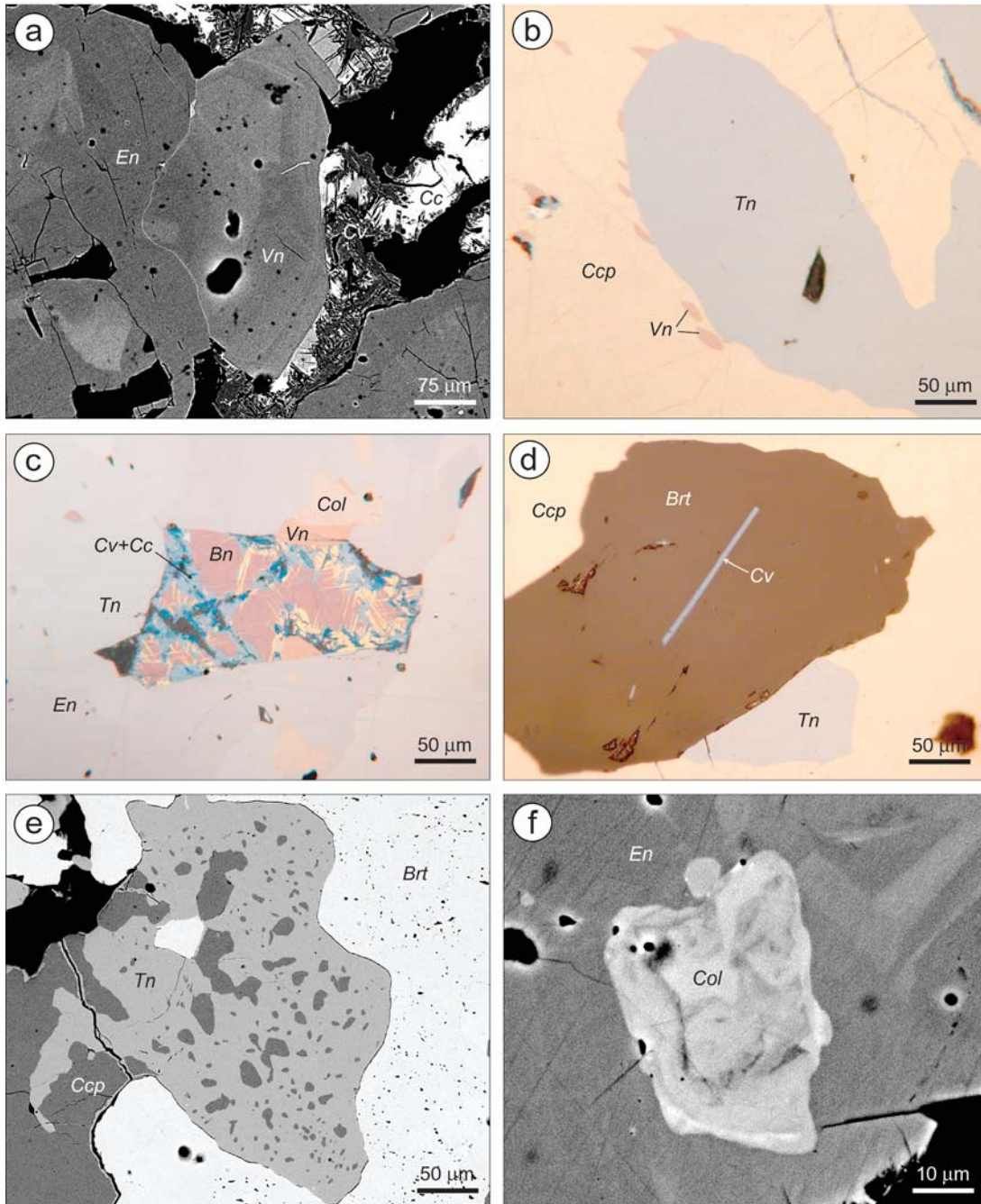


FIG. 5. Mineralogy of the vinciennite-bearing Cu-As-Sn assemblage in the Radka deposit. a) Zoned crystal of vinciennite (Vn) in the interstice of an aggregate of enargite (En). Chalcopyrite (Ccp) is altered to chalcocite (Cc) and covellite (Cv). Back-scattered electron (BSE) image. b) Vinciennite crystals formed at the contact between tennantite (Tn) and chalcocite replacing enargite (En). Photomicrograph in reflected light (parallel nicols). c) Secondary assemblage of bornite (Bn) – chalcocite – covellite replacing chalcopyrite in association with enargite, tennantite, vinciennite and colusite (Col). Photomicrograph in reflected light (partly crossed nicols). d) Tabular crystal of covellite included in barite (Brt) surrounded by chalcopyrite and tennantite. Photomicrograph in reflected light (parallel nicols). e) Chalcopyrite–tennantite symplectitic intergrowth texture. BSE image. f) Inclusion of zoned colusite in enargite crystal. BSE image.

diagram (Fig. 9). Copper in excess, after subtraction of 10 Cu atoms, is presented as Cu^* . The tennantite at Radka plots in two fields of the diagram. For one part of the tennantite samples, all Fe is as Fe^{3+} , which is compensated by Cu^+ (lower field on Figure 9). Most data points (>85%) plot in the upper part of the diagram, together with the tennantite from Layo, Chizeuil and two samples from Huaron. The latter field corresponds to tennantite with an excess of copper that is not compensated by Fe^{3+} , thus indicating possible presence of Cu^{2+} , which requires an absence of Fe^{2+} . The possibility, mentioned by Marcoux *et al.* (1994), that some Cu^+ can occupy interstitial sites in the structure on the basis of the low $[\text{As} + \text{Sb}]$ total, is not acceptable for the Radka tennantite, where $[\text{As} + \text{Sb}]$ is nearly stoichiometric (average value of 3.99 *apfu*; Table 1).

Marcoux *et al.* (1994) suggested that in vinciennite, $\text{Cu}_{10}\text{Fe}_4\text{SnAsS}_{16}$, iron is also in the Fe^{3+} state and some of the Cu atoms probably are divalent, thus transforming the empirical formula to $\text{Cu}^+_9\text{Cu}^{2+}\text{Fe}^{3+}_4\text{Sn}^{4+}\text{As}^{5+}\text{S}^{2-}_{16}$. Jambor & Owens (1987) noted that not only Cu but also Fe in vinciennite is probably heterovalent, suggesting that at least one of the iron atoms is divalent. As the structure of vinciennite has not been solved yet [Cesbron *et al.* (1985) described it as tetragonal $P4_122$, or possibly $P4/mmm$, $P422$ or $P4mm$], its stoichiometry is still speculative. Spry *et al.* (1994) proposed the formula $\text{Cu}_{11}\text{Fe}_4\text{SnAsS}_{16}$, rather than the original formula estab-

lished by Cesbron *et al.* (1985). They argued that the new formula was in better agreement with the analytical data; with this new formulation, the heterovalency of Fe, claimed by Jambor & Owens (1987), is no longer necessary.

Electron-microprobe data for vinciennite from the Radka deposit, together with published data from other localities, are reported on a Cu *versus* Fe diagram (Fig. 10a). The very good negative correlation between Cu in excess after subtraction of 10 Cu atoms and Fe suggests that at least one atom of Fe is divalent and substitutes for one atom of Cu (most probably Cu^{2+}). The slight deviation from the theoretical trend of such a substitution toward higher values (Fig. 10a) is consistent with the slight cationic excess over the stoichiometric composition, already mentioned by previous investigators. A particular feature of the vinciennite from Radka is the substitution of Ge for Sn (Fig. 10b) and of some minor Sb for As. On the basis of the new results concerning the crystal chemistry of vinciennite and in agreement with the original formula of Cesbron *et al.* (1985), calculated on the basis of 16 cations, we propose a new formula that best describes the substitutions in vinciennite involving heterovalency of copper and iron: $\text{Cu}^+_8\text{Cu}^{2+}_2\text{Fe}^{3+}_3(\text{Fe,Cu})^{2+}(\text{Sn,Ge})^{4+}(\text{As,Sb})^{5+}\text{S}^{2-}_{16}$.

Within the deposits from the Panagyurishte district, coltsite has been described in the porphyry copper deposits of Medet (Strashimirov 1982) and Assarel

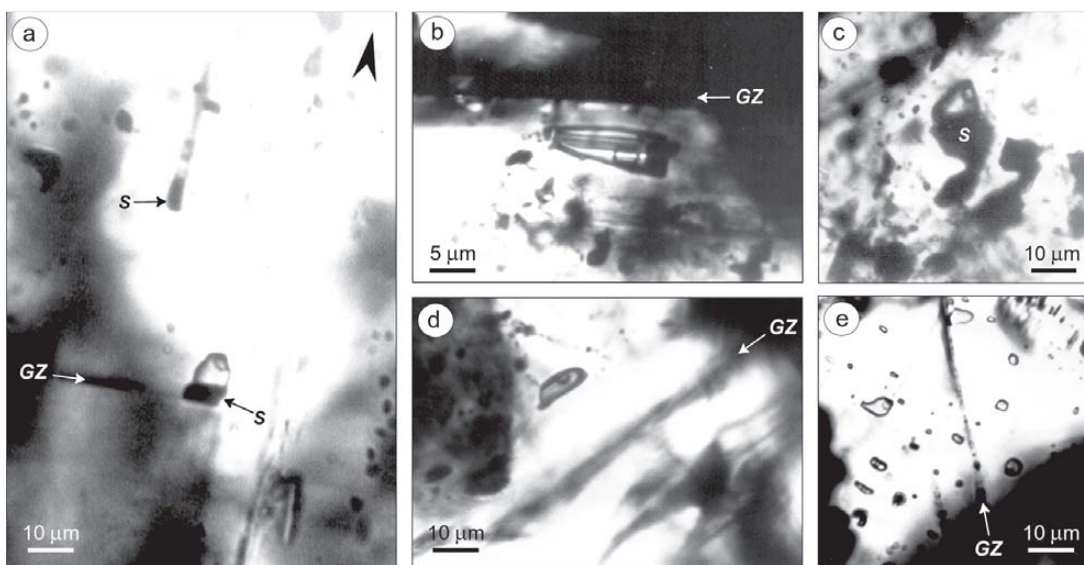


FIG. 6. Enargite-hosted fluid inclusions from the Radka deposit. Microphotographs in infrared transmitted light. a) Isometric and channel-like primary fluid inclusions attached to solids (S) trapped in growth zones (GZ) of enargite. The small arrow indicates direction of crystal growth (see text for explanation). b) Flat elongate primary fluid inclusion parallel to growth zone. c) Primary fluid inclusion attached to solid in the central part of enargite crystal. d) Isolated primary inclusion parallel to growth zone. e) Secondary fluid inclusion plane cross-cutting a growth zone. Note the same vapor:liquid ratio in different inclusions from this plane.

(Petrunov *et al.* 1991), and in the high-sulfidation copper–gold deposit of Chelopech (Terziev 1966, Petrunov 1994). A specific aspect of the colusite from the Cu–As–Sn assemblage in Radka is its Ge content (Fig. 11). As in vinciennite, iron and copper are probably divalent in colusite from Radka. Vanadium is replaced by Fe³⁺, for a total of 2 [V + Fe³⁺] atoms, and the rest of the iron (most likely Fe²⁺) substitutes for Cu²⁺ (Table 3). Kovalenker *et al.* (1984) suggested a similar scheme of substitution for nekrasovite, the tin end-member of the colusite series: Cu⁺₁₈(Cu,Fe,Zn)²⁺₈(V,Fe)³⁺₂(Sn⁴⁺, As⁵⁺, Sb⁵⁺)₆S²⁻₃₂.

The mineral chemistry of the main ore minerals from the vinciennite-bearing Cu–As–Sn (± Au) assemblage at Radka implies very particular conditions of ore formation, comparable with those in the Layo epithermal

deposit (Marcoux *et al.* 1994). The precipitation of As as As⁵⁺ in enargite, vinciennite and colusite, and As³⁺ in tennantite, and the deposition of minor covellite at the beginning of the stage, indicate generally high activity of sulfur in the fluid phase (Hayba *et al.* 1985), which is decreasing with time (enargite to tennantite transformation). Fluids were mildly acidic, with a pH of 4.5–5.5 based on illite stability at 250°C (Heald *et al.* 1987). The high activity of sulfur probably also favored the fixation of Fe exclusively as Fe³⁺ in tennantite, vinciennite and colusite. The fluids were completely depleted in Zn, but slightly enriched in Ge, which was incorporated as a trace element in vinciennite and colusite. These two elements, together with Sb and Ag, were deposited during the later stages of mineralization, especially stages IV and V (Fig. 2). Such an evolution

TABLE 2. COMPOSITION OF VINCIENNITE FROM THE RADKA DEPOSIT, BULGARIA

	1	2	3	4	5	6	7	8	9	10	11	12	
Cu wt.%	45.00	44.83	46.24	45.77	43.30	43.08	43.36	42.01	42.24	42.26	42.44	42.63	
Fe	12.15	11.76	11.99	12.21	13.71	12.59	12.57	14.24	14.16	14.00	12.82	13.09	
Sn	6.35	6.29	6.94	7.05	7.51	6.99	6.97	7.61	7.65	7.56	6.70	6.20	
As	4.42	4.60	3.98	3.91	4.29	4.43	4.32	4.27	4.37	4.37	3.92	3.89	
Sb	0.43	0.54	0.45	0.42	0.36	0.36	0.42	0.60	0.54	0.43	0.97	1.07	
Ge						0.19	0.21				0.42	0.72	
S	31.66	31.08	29.93	30.21	31.24	30.73	31.08	30.26	30.70	30.52	31.13	31.03	
Total	100.01	99.10	99.53	99.57	100.41	98.37	98.93	98.99	99.66	99.14	98.40	98.63	
Cu <i>apfu</i>	10.88	10.91	11.01	10.93	10.38	10.56	10.60	10.15	10.17	10.22	10.48	10.44	
Fe	3.34	3.26	3.25	3.32	3.74	3.51	3.50	3.92	3.88	3.85	3.60	3.65	
Sn	0.82	0.82	0.88	0.90	0.96	0.92	0.91	0.98	0.99	0.98	0.89	0.81	
As	0.91	0.95	0.80	0.79	0.87	0.92	0.89	0.88	0.89	0.90	0.82	0.81	
Sb	0.1	0.07	0.06	0.05	0.05	0.05	0.05	0.08	0.07	0.05	0.13	0.14	
Ge						0.04	0.04				0.09	0.15	
S	15.2	14.99	14.12	14.30	14.84	14.93	15.06	14.49	14.66	14.63	15.23	15.06	
Σcat/S	1.05	1.07	1.13	1.12	1.08	1.07	1.06	1.10	1.09	1.09	1.05	1.06	
	13	14	15	16	17	18	19	20	21	22	23	24	Ave.
Cu wt.%	42.60	43.50	42.66	43.20	42.62	42.66	42.65	42.27	42.70	42.72	42.62	42.66	43.17
Fe	13.10	12.36	12.73	12.84	12.88	12.86	12.99	12.72	12.25	13.04	13.00	12.91	12.87
Sn	6.37	6.95	6.13	6.45	5.31	6.48	5.61	7.21	6.59	6.89	7.65	6.92	6.77
As	4.00	3.82	3.83	4.03	4.16	3.91	3.97	3.84	3.87	4.00	3.79	4.11	4.09
Sb	0.90	1.14	1.17	1.01	0.95	1.16	0.91	1.15	1.06	1.12	1.23	1.09	0.81
Ge	0.87	0.20	0.71	0.66	1.32	0.38	0.98	0.32	0.56	0.29		0.20	0.33
S	31.45	30.84	31.29	31.16	31.11	30.80	30.95	30.80	31.05	30.94	31.24	30.96	30.92
Total	99.29	98.81	98.52	99.35	98.35	98.25	98.06	98.31	98.08	99.00	99.53	98.85	98.96
Cu <i>apfu</i>	10.40	10.66	10.51	10.51	10.44	10.50	10.48	10.45	10.59	10.44	10.43	10.46	10.35
Fe	3.64	3.45	3.57	3.55	3.59	3.60	3.63	3.58	3.46	3.63	3.62	3.60	3.74
Sn	0.83	0.91	0.81	0.84	0.70	0.85	0.74	0.95	0.88	0.90	1.00	0.91	0.92
As	0.83	0.79	0.80	0.83	0.86	0.82	0.83	0.81	0.81	0.83	0.79	0.85	0.84
Sb	0.11	0.15	0.15	0.13	0.12	0.15	0.12	0.15	0.14	0.14	0.16	0.14	0.09
Ge	0.18	0.04	0.15	0.14	0.28	0.08	0.21	0.07	0.12	0.06		0.04	0.06
S	15.22	14.98	15.29	15.02	15.11	15.02	15.07	15.09	15.26	14.98	15.16	15.04	15.14
Σcat/S	1.05	1.07	1.05	1.06	1.06	1.07	1.06	1.06	1.05	1.07	1.06	1.06	1.06

The empirical formula is calculated on the basis of Σcations = 16 atoms per formula unit (*apfu*).

TABLE 3. REPRESENTATIVE COMPOSITIONS OF COLUSITE FROM THE RADKA DEPOSIT, BULGARIA

	1	2	3	4	5	6	7	8	9	10	11	Ave.
Cu wt.%	48.55	48.96	49.28	48.98	49.02	48.51	48.05	48.29	48.73	49.11	49.56	48.82
Fe	1.38	1.14	1.77	1.94	0.74	0.88	1.43	0.53	1.46	0.44	0.55	1.11
V	2.34	2.27	1.94	2.27	2.56	2.53	2.13	2.51	2.09	2.72	2.55	2.36
As	8.54	8.52	9.35	8.23	7.90	7.85	7.79	6.76	7.67	8.82	7.78	8.11
Sn	5.07	5.97	4.00	5.49	5.88	6.53	7.00	6.77	6.69	4.40	5.58	5.76
Sb	1.47	1.55	1.22	1.41	2.36	2.19	1.93	3.92	1.92	1.65	2.85	2.04
Ge	1.09	0.51	1.14	0.83	0.33	0.21			0.22	0.89	0.32	0.50
S	30.47	30.49	30.54	30.65	30.57	30.00	30.43	29.78	30.42	30.89	30.67	30.45
Total	98.91	99.41	99.24	99.80	99.36	98.70	98.76	98.56	99.20	98.92	99.86	99.15
Cu <i>apfu</i>	25.72	25.93	26.05	25.80	25.89	26.10	25.49	26.18	25.86	25.66	26.09	25.72
Fe	0.83	0.69	1.06	1.17	0.45	0.54	0.87	0.32	0.88	0.26	0.33	0.83
V	1.55	1.50	1.28	1.49	1.69	1.70	1.41	1.69	1.39	1.77	1.68	1.55
As	3.84	3.83	4.19	3.68	3.54	3.58	3.51	3.11	3.45	3.91	3.47	3.84
Sn	1.44	1.69	1.13	1.55	1.66	1.88	1.99	1.96	1.90	1.23	1.57	1.44
Sb	0.41	0.43	0.34	0.39	0.65	0.62	0.53	1.11	0.53	0.45	0.78	0.41
Ge	0.50	0.24	0.53	0.38	0.15	0.10			0.10	0.41	0.15	0.50
S	32.00	32.00	32.00	32.00	32.00	32.00	32.00	32.00	32.00	32.00	32.00	32.00

The concentration of Zn is systematically below the detection limit of the electron microprobe: 0.10 wt.%. The empirical formulae were calculated on the basis of 32 atoms of S per formula unit (*apfu*).

TABLE 4. SUMMARY OF HOMOGENIZATION, FREEZING, AND DISSOLUTION TEMPERATURES FOR FLUID INCLUSIONS IN ENARGITE AND QUARTZ PHENOCRYSTS FROM THE RADKA DEPOSIT, BULGARIA

Host mineral	Type	Origin	T _{h,L-V} range mean (°C)	n	T _{m,ice} range mean (°C)	n	T _{m,NaCl} range mean (°C)	n	Salinity wt.% eq. NaCl
Enargite	L-V	P	235–304 249	18	-6.8–-6.4 -6.5	13			9.7–10.2 9.9
	L-V	S	223–245 229	4	-6.7–-6.3 -6.5	2			9.6–10.1 9.9
Quartz pheno- crysts	L-V	S	296–323 311	23	-2.8–-1.6 -2.0	22			2.7–4.6 3.4
	L-V-S	S	70–264 195	15			185–386 245	15	31.2–46.0 34.7

Types of inclusion: L-V: two-phase liquid-rich; L-V-S: three-phase liquid + vapor + halite. Origin of inclusions: P: primary, S: secondary. The salinity of the trapped fluid was calculated from either the temperature of final melting of ice (Bodnar 1993), or from the dissolution temperature of halite (Sterner *et al.* 1988). T_{h,L-V}: temperature of homogenization; T_{m,ice}: final temperature of ice melting; T_{m,NaCl}: dissolution temperature of halite.

of the hydrothermal system with time is characteristic of some classic examples of late-magmatic mineralization related to porphyry copper systems (Einaudi 1977). As tin is an element commonly enriched in porphyry-type deposits (Sillitoe *et al.* 1975), the Sn signature of the assemblage studied is another argument in favor of a possible genetic link with a porphyry system at Radka.

Fluid evolution at Radka

Suitable hosts for fluid-inclusion studies are scarce in high-sulfidation epithermal deposits, as the gangue minerals are typically fine-grained (Arribas 1995). The most reliable data on the ore-forming fluids are obtained using infrared microscopy directly on ore minerals such as enargite (Campbell *et al.* 1984). Microthermometric studies on enargite-hosted fluid inclusions from several

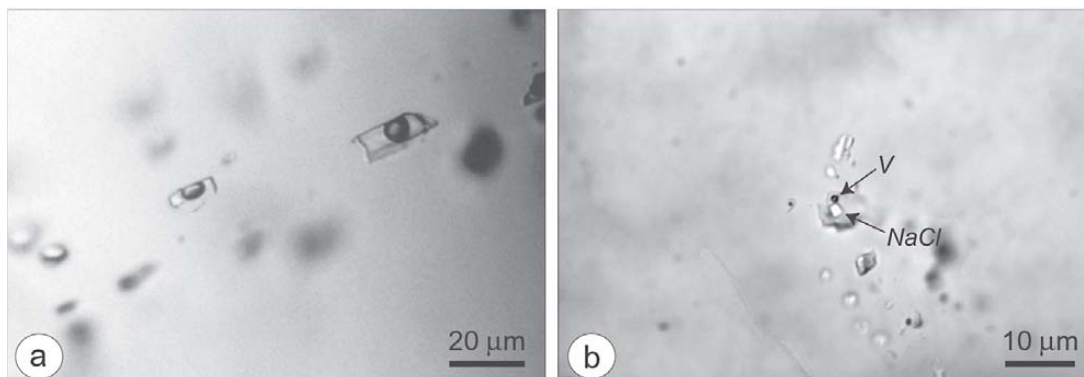


FIG. 7. Fluid inclusions in quartz phenocrysts. a) Two-phase (L-V) fluid inclusions. b) Three-phase (L-V-NaCl) inclusion.

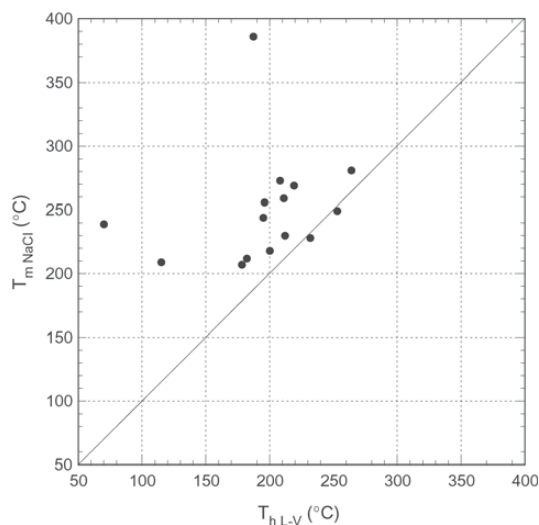


FIG. 8. Halite dissolution temperatures ($T_{m \text{ NaCl}}$) versus temperature of vapor bubble disappearance ($T_{h \text{ L-V}}$) for individual halite-saturated inclusions in quartz phenocrysts from dacitic host-rock at Radka. The $T_{h \text{ L-V}} = T_{m \text{ NaCl}}$ line separates inclusions that undergo final homogenization by halite dissolution from those that homogenize by disappearance of vapor bubble.

high-sulfidation deposits [Lepanto, Philippines: Mancano & Campbell (1995); Julcani, Peru: Deen *et al.* (1994); Chelopech, Bulgaria: Moritz *et al.* (2002)] strongly support the idea that hydrothermal solutions responsible for the enargite precipitation are the result of mixing between two end-member fluids: a) a high-temperature and high-salinity parent magmatic fluid, and b) a low-temperature, low-salinity fluid, most likely groundwater (Arribas 1995).

Most genetic models for high-sulfidation epithermal deposits (*e.g.*, Hedenquist *et al.* 1998, Shinohara & Hedenquist 1997) stress an early stage of advanced argillic alteration (quartz-alunite ledge formation) associated with the absorption of high-pressure magmatic vapor by deep meteoric water, resulting in the formation of highly reactive acidic waters in an environment shallower than the porphyry one. On the basis of studies of active high-sulfidation epithermal systems [*e.g.*, White Island: Hedenquist *et al.* (1993); Satsuma Iwojima: Hedenquist *et al.* (1994)] and their fossil analogues [*e.g.*, Lepanto: Hedenquist *et al.* (1998)], Hedenquist and his colleagues proposed that the most widespread low-salinity (2–4 wt.% equiv. NaCl) fluids in these deposits are related to the relatively later stage of alteration to white mica, usually formed after the formation of advanced argillic alteration lithocaps in the central parts of the magmatic-hydrothermal system, and that they are the main ore-precipitating fluids. As reported by Hedenquist & Richards (1998), “sericitic” alteration forms from waters that have a magmatic signature, with variable isotopic compositions ranging from >90% end-member magmatic to about 3:1 mixtures of magmatic and meteoric water.

Muntean & Einaudi (2001) proposed an alternative scenario for the fluids responsible for the high-sulfidation epithermal mineralization in the Maricunga belt, northern Chile. They assumed that both enargite-bearing ore and surrounding quartz-alunite alteration formed at essentially the same time from a late supercritical magmatic fluid with a salinity of 10 wt.% NaCl (salinity considered appropriate for supercritical magmatic fluids; *cf.* Hedenquist *et al.* 1998). The fluid cooled below its critical temperature without entering the two-phase liquid + vapor field. Upon crossing into the brittle regime (<400°C) at depths of about 2 to 3 km, the fluid underwent abrupt decompression and boiled along the liquid + vapor curve under hydrostatic

pressure. Such a boiling did not generate a hypersaline liquid, but caused a progressive and moderate increase in the salinity of the liquid phase (Fournier 1987). Ore was deposited from the liquid phase, while the condensation of magmatic volatiles (*e.g.*, SO_2 , HCl) into shallow meteoric water above the ascending liquid resulted in “sericitic” alteration at depth and quartz–alunite and vuggy quartz near the surface (Muntean & Einaudi 2001).

Heinrich *et al.* (1999) suggested another possibility for the accumulation of low-salinity (< ~10 wt.%) fluids in the high-sulfidation epithermal environment. They proposed cooling of a magmatic vapor at elevated pressure or its condensation into nonmagmatic water at lower temperature in the deeper part of the magmatic–hydrothermal system, transitional between the porphyry and the epithermal zone, without additional input of superficial meteoric waters. This hypothesis is based on the preferential enrichment of Cu, Au, As and S into low-density inclusions of magmatic vapor relative to

coexisting brine inclusions, observed by LA–ICP–MS micro-analysis in the Grasberg porphyry Cu–Au deposit, in the Irian Jaya Mountains of Indonesia. Thus, the vapor-like low- to intermediate-salinity fluids could be the prime agent for selective transfer of ore metals into the high-sulfidation epithermal deposits. Recently, Heinrich (2003) provided thermodynamic constraints on the mechanism of transport of ore metals by low-density magmatic fluid, and demonstrated that such a fluid originating either by direct exsolution from a silicate melt or by separation of vapor from a high-temperature brine (>400°C), can cool and condense to an aqueous liquid without further phase transition.

Data on fluid-inclusion microthermometry for the Radka deposit are summarized in Figure 12. The halite-saturated solution in the secondary inclusions in quartz phenocrysts may be derived from either of two processes, injection of an exotic magmatic brine into the shallow part of the system, or entrapment during almost complete (up to 99%) vaporization of a deeply derived,

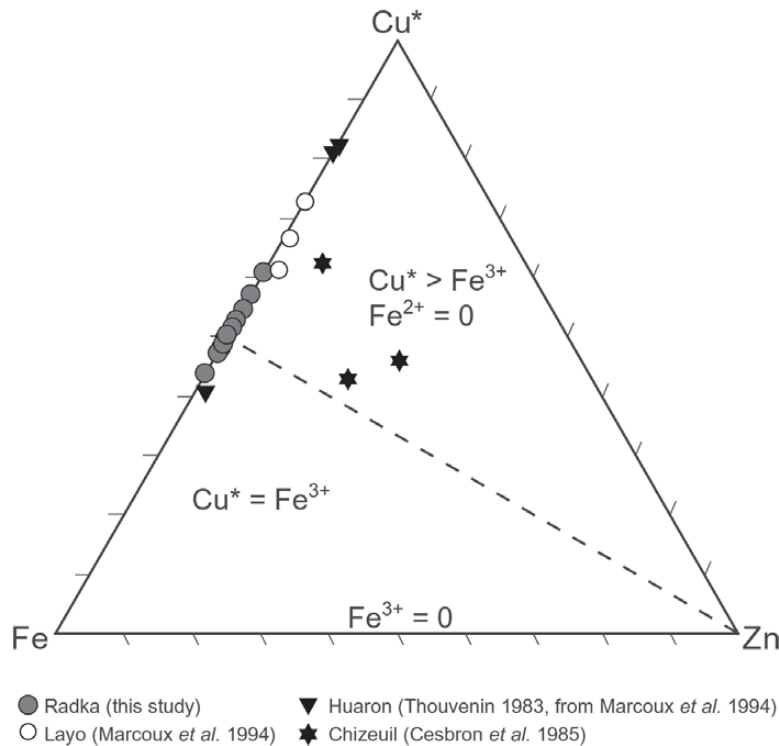


FIG. 9. Compositions of Cu-excess tennantite in association with vinciennite from different localities plotted in the Cu–Fe–Zn system (*apfu*). Cu^* is Cu in excess after subtraction of $10(\text{Cu} + \text{Ag})$ atoms for a total of 12 metal atoms. Lower field ($\text{Cu}^* = \text{Fe}^{3+}$) includes compositions where excess Cu is compensated by Fe^{3+} . Upper field includes compositions where Cu^* is not compensated by Fe^{3+} ($\text{Cu}^* > \text{Fe}^{3+}$), which is an indication of Cu^{2+} , requiring an absence of Fe^{2+} .

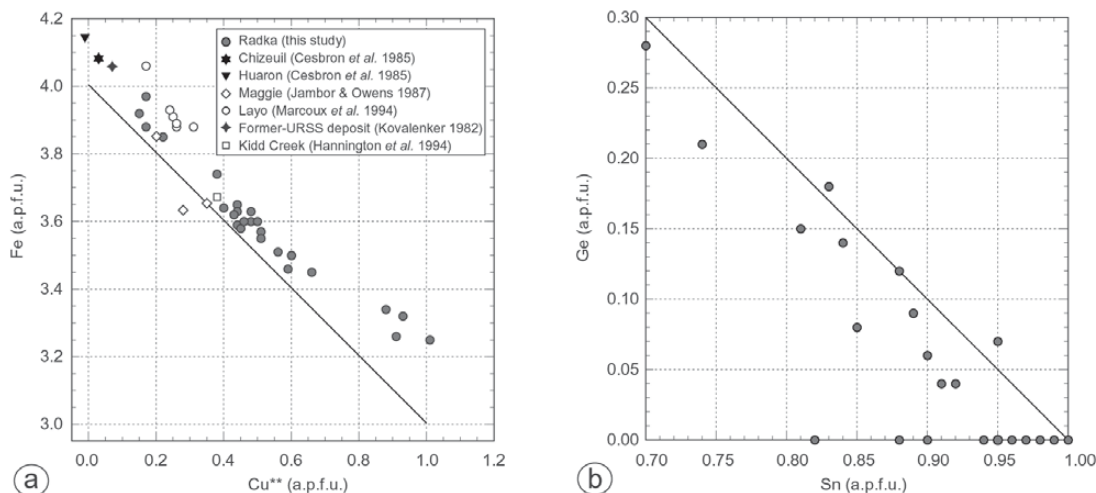


FIG. 10. a) Cu^{**} versus Fe diagram (apfu) showing vinciennite compositions from various localities. Cu^{**} is Cu in excess after subtraction of 10 Cu atoms for a total of 16 cations. The black line corresponds to the theoretical trend of substitution of 1 Cu excess atom for 1 Fe atom. b) Sn versus Ge diagram (apfu) showing vinciennite compositions from Radka. The line corresponds to the theoretical substitution trend of Ge for Sn.

dilute thermal water, as has been proposed by Simmons & Browne (1997) for secondary saline fluid inclusions in sphalerite from the Broadlands–Ohaaki geothermal system. A sedimentary origin of these brines can be excluded because there are no evaporite sequences within the Panagyurishte ore zone that may explain the saline nature of such fluids.

The restricted ranges of T_h and salinity of the enargite-hosted fluid inclusions characterize the Cu–As–Sn assemblage at Radka as a single hydrothermal event, differing from the other stages of mineralization. We believe that the enargite-precipitating fluid had an intermediate position between the hypothetical magmatic brines, represented by NaCl-saturated inclusions in quartz phenocrysts, and the most widespread relatively low-salinity (3–5 wt.% equiv. NaCl) fluids, determined for the main stages of mineralization at Radka (Fig. 12). Two alternative scenarios are possible to explain the intermediate salinity of enargite-precipitating fluids. The first one (path A, Fig. 12) consists in a direct magmatic input to the hydrothermal system at Radka, either by a supercritical magmatic fluid, as proposed by Muntean & Einaudi (2001) for the deposits of the Maricunga belt, in Chile, or by a condensed magmatic vapor-like fluid, as proposed by Heinrich (2003). The salinity of ~10 wt.% NaCl of the enargite-forming fluids strongly supports either hypothesis. The second scenario (path B, Fig. 12) involves a mixture of hot magmatic brine and low-salinity water. This scenario is more consistent with the mixing trends observed in other

high-sulfidation epithermal deposits (e.g., Moritz *et al.* 2002), but does not fit very well with the very restricted range of salinities and T_h registered for the enargite-hosted fluid inclusions at Radka. Both scenarios favor the dominantly magmatic signature of the fluid responsible for the formation of the Cu–As–Sn assemblage. The salinity of the “diluted” fluids at Radka is restricted to 3 to 5.5 wt.% equiv. NaCl, thus supporting the “magmatic vapor condensation” model (Heinrich 2003) under lithostatic pressure (see below), or more important mixing between magmatic fluid and deep groundwater (Arribas 1995). However, to be able to quantify correctly the magmatic input to the ore-forming fluids in the Radka deposit, further stable isotopic analyses of inclusion fluids are needed, especially in sulfide minerals, such as enargite and pyrite, which are not susceptible to ^{18}O exchange between fluid-inclusion waters and host (cf. Deen *et al.* 1994).

An important feature of the fluid evolution at Radka is the increase of T_h , up to 365°C, registered for a nearly constant salinity of the fluids for the late quartz–pyrite vein assemblage [Si–Fe (\pm Co) stage VI, Fig. 12]. A possible explanation for this process consists of late pulses of high-pressure magmatic vapor ascending from and condensing above a deeper porphyry system (Kouzmanov *et al.* 2002). Sulfur isotope data ($\Delta^{34}\text{S} \approx 0\text{‰}$) for the late cobalt-bearing pyrite are in agreement with such a hypothesis. The late anhydrite-bearing (Ca \pm Fe) assemblage was formed by oxidized and cooler fluids at 230–180°C (Strashimirov & Kovachev 1992).

The vincienite-bearing Cu–As–Sn assemblage in the high-sulfidation epithermal environment: metallogenic implications

Most of the ore deposits in which a vincienite-bearing assemblage has been described show features of high-sulfidation epithermal systems (*i.e.*, Lemiere *et al.* 1986, Marcoux *et al.* 1994). Jambor & Owens (1987) described vincienite from quartz – pyrite – tennantite veinlets peripheral to the main ore zone at the Maggie porphyry copper – molybdenum deposit in British Columbia, corresponding probably to the transition zone to the epithermal part of the magmatic–hydrothermal system (Hedenquist *et al.* 1998).

The geology of the Radka deposit, its mineralogical and geochemical particularities, ore textures, type of hydrothermal alterations and the character of the fluids, allow us to define the deposit as a deep part of a high-sulfidation epithermal system, possibly related to a porphyry copper system (Hedenquist & Lowenstern 1994,

Sillitoe 1999). Another argument supporting this conclusion is the maximum depth of formation of the Radka deposit, estimated to be ~2 km, based on the microthermometry study of fluid inclusions in pyrite (Kouzmanov *et al.* 2002).

The mineralogical and geochemical features of the vincienite-bearing Cu–As–Sn (\pm Au) assemblage in the Radka deposit are very similar to those at Layo (Marcoux *et al.* 1994) and Chizeuil (Cesbron *et al.* 1985). The high activity of sulfur and the oxidized and slightly acidic character of the fluids are other points in common. In Radka, the IR microthermometry of enargite-bearing fluid inclusions allowed us to determine the temperature of formation of this assemblage. If the measured T_h of 250°C of fluid inclusions with a salinity of 9.9 wt.% equiv. NaCl is corrected for an estimated maximum pressure of trapping of 430 bar at Radka (Kouzmanov *et al.* 2002), we obtain a temperature of formation of about 275°C. This temperature is very close to 280°C, the lowest temperature of stability of Sb-free enargite (the high-temperature modification of Cu_3AsS_4 ; Maske & Skinner 1971, Posfai & Buseck 1998). At Radka, the low-temperature modification, luzonite, which is stable below 280°C, was not observed. The enargite contains minor Sb (up to 1.5 wt.%), which increases slightly the temperature of the phase transition (Posfai & Buseck 1998).

Paragenetic relations in the Cu–As–Sn assemblage studied at Radka indicate an evolution to a lower sulfidation state with time, from enargite to tennantite–chalcopyrite deposition. This tendency is preserved during the stages 4 and 5, when a base-metal mineralization formed, accompanied by Au (Fig. 2). The paragenesis at Radka is similar to that in the Chelopech high-sulfidation epithermal deposit, in the northern part of the Panagyurishte district (Petrunov 1994). The shift to a lower sulfidation state with time is accompanied by less acidic conditions and an increase in the oxidation state of the fluids, illustrated by massive formation of anhydrite veins during the latest Ca \pm Fe stage of mineralization.

Copper, sulfur and arsenic are the characteristic major elements determining the geochemical signature not only of the studied vincienite-bearing assemblage, but also of the Radka deposit in general. In a porphyry environment, as demonstrated by Heinrich *et al.* (1999), these elements are preferentially concentrated into the vapor phase during separation of the parental magmatic fluid to give a liquid brine and a low-density vapor. The low-density magmatic gas-like fluids have a significant metal-transporting capacity (*e.g.*, Lowenstern *et al.* 1991, Williams-Jones *et al.* 2002) and could play a substantial role in the formation of high-sulfidation ore deposits, as proposed by Heinrich (2003).

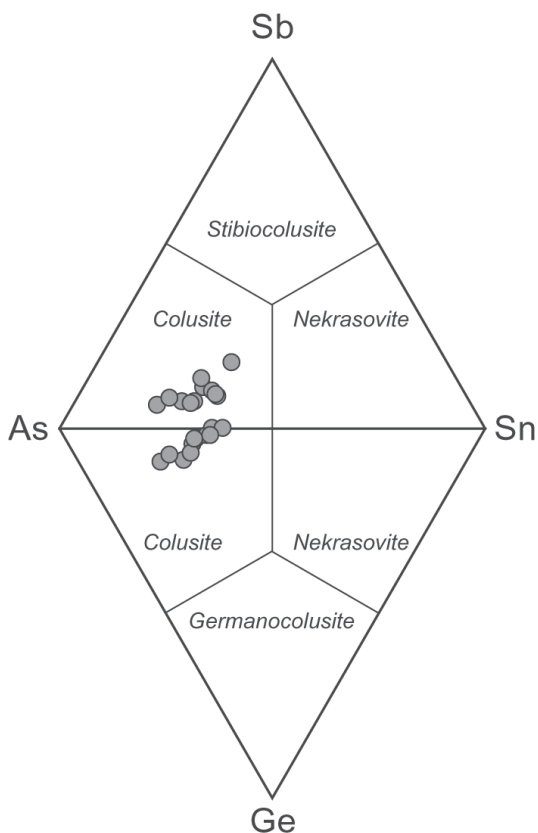


FIG. 11. Compositions of colusite from the Radka deposit, projected in the As–Sn–Sb–Ge diagram.

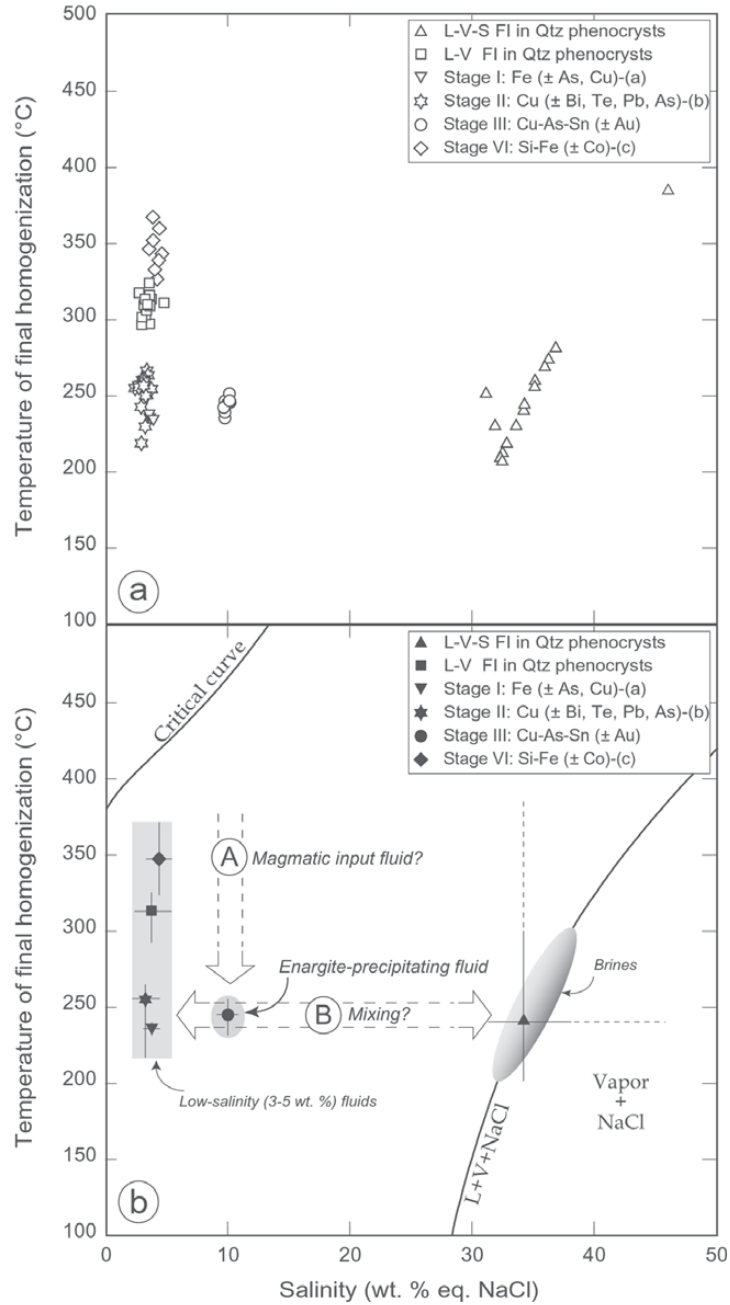


FIG. 12. Temperatures of final homogenization *versus* salinity diagram for fluid inclusions in Radka. a) Measurements on single fluid inclusions. Data are from (a) Kouzmanov (2001), (b) Kouzmanov *et al.* (2000a), (c) Kouzmanov *et al.* (2002), and this study. b) Interpretive diagram for the origin of enargite-precipitating fluid at Radka. Data points correspond to modal values for different stages of mineralization presented in a). Error bars indicate the range of data. The paths labeled A and B refer to the proposed two fluid paths responsible for the formation of the Cu–As–Sn assemblage in Radka, as explained in the text. The critical curve is from Driesner & Heinrich (2002), and the solubility curve (L + V + NaCl) is from Sourirajan & Kennedy (1962).

CONCLUSIONS

Our systematic mineralogical, trace element and fluid-inclusion study of the vincienite-bearing Cu–As–Sn (\pm Au) assemblage from the Radka copper epithermal deposit, Bulgaria, reveals physicochemical parameters of formation very similar to those inferred for analogous deposits in other parts of the world. This assemblage was formed by oxidized and slightly acidic fluids, with a high fugacity of sulfur and an intermediate salinity at a temperature of about 275°C, typical features for high-sulfidation epithermal systems (Hedenquist & Arribas 1999, Hedenquist *et al.* 2000). The geology of the Radka deposit, its geochemical peculiarities, ore textures and patterns of hydrothermal alteration, complemented by the new results about the mineralogical features and the nature of the hydrothermal fluids, allow us to interpret the deposit as a deep part of a high-sulfidation epithermal system, possibly related to a porphyry copper system, which is consistent with the close spatial and genetic relationship between epithermal and porphyry-copper deposits in the Panagyurishte ore region (Popov & Popov 1997, Strashimirov *et al.* 2002).

The detailed electron-microprobe study of vincienite and associated minerals at Radka reveals the heterovalency of Cu and Fe in minerals from this assemblage. The tennantite associated with vincienite, as a rule, corresponds to “Cu-excess” tennantite (Marcoux *et al.* 1994). New data on the composition of vincienite led us to elucidate some aspects of its crystal chemistry (such as incorporation of Cu^{2+} and Fe^{3+} and $\text{Sn}^{4+} \rightleftharpoons \text{Ge}^{4+}$ substitution), obviously strongly dependent on the physicochemical parameters of formation. Thus vincienite, a rare Sn-bearing sulfide, with only seven known occurrences in the world, forms in a geological environment typical of the transition zone between porphyry to epithermal deposits, in particular, conditions within a uniform mineral assemblage including enargite, Cu-excess tennantite, chalcopyrite and additional Sn-bearing minerals.

ACKNOWLEDGEMENTS

The authors thank Dimitar Tsonev for providing some samples from the deep levels of exploitation in the Radka deposit, Vsevolod Kourtchatov for giving us access to the collection of the Mineralogy and Petrography Museum of the University of Sofia, Annick Genty for her assistance during the scanning electron microscopy, and Olivier Rouer for his help with the electron-microprobe analyses. We are indebted to Yves Moëlo, Robert Moritz, Ivan Bonev and Chris Heinrich for fruitful discussions and advice. We thank Volker Lüders and Robert Moritz for helpful reviews of the manuscript. The study was supported by ISTO–CNRS Orléans, BRGM Orléans and a grant to KK by the Ministère des Affaires Étrangères, France. This is a contribution to the

GEODE (European Science Foundation) program “Geodynamics and Ore Deposit Evolution of the Alpine – Balkan – Carpathian – Dinaride Province”.

REFERENCES

- ARRIBAS, A., JR. (1995): Characteristics of high-sulfidation epithermal deposits, and their relation to magmatic fluid. *In* *Magma, Fluids, and Ore Deposits* (J.F.H. Thompson, ed.). *Mineral. Assoc. Can., Short Course Vol. 23*, 419-454.
- BERZA, T., CONSTANTINESCU, E. & VLAD, S.-N. (1998): Upper Cretaceous magmatic series and associated mineralisation in the Carpathian–Balkan region. *Resource Geol.* **48**, 291-306.
- BODNAR, R.J. (1993): Revised equation and table for determining the freezing point depression of H_2O –NaCl solutions. *Geochim. Cosmochim. Acta*, **57**, 683-684.
- BOGDANOV, B. (1980): Massive sulphide and porphyry copper deposits in the Panagjurishte district, Bulgaria. *In* *European Copper Deposits* (S. Jankovic & H.R. Sillitoe, eds.). *Soc. Geology Applied to Mineral Deposits (SGA), Spec. Publ.* **1**, 50-58.
- , BOGDANOVA, R. & CHIPCHAKOVA, S. (1970): Intrusive ore breccias from the Radka and Elshitsa deposits in the Panagyurishte ore district. *Rev. Bulg. Geol. Soc.* **31**(1), 97-101 (in Bulg.).
- CAMPBELL, A.R., HACKBARTH, C.J., PLUMLEE, G.S. & PETERSEN, U. (1984): Internal features of ore minerals seen with the infrared microscope. *Econ. Geol.* **79**, 1387-1392.
- CESBRON, F., GIRAUD, R., PICOT, P. & PILLARD, F. (1985): La vincienite $\text{Cu}_{10}\text{Fe}_4\text{Sn}(\text{As},\text{Sb})\text{S}_{16}$, une nouvelle espèce minérale. Etude paragenétique du gîte type de Chizeuil, Saône-et-Loire. *Bull. Minéral.* **108**, 447-456.
- CHARLAT, M. & LÉVY, C. (1974): Substitutions multiples dans la série tennantite–tétrahédrite. *Bull. Soc. fr. Minéral. Cristallogr.* **97**, 241-250.
- CHARNOCK, J.M., GARNER, C.D., PATTRICK, R.A.D. & VAUGHAN, D.J. (1989): EXAFS and Mössbauer spectroscopic study of Fe-bearing tetrahedrites. *Mineral. Mag.* **53**, 193-199.
- CHIPCHAKOVA, S., KARADJOVA, B., ANDREEV, A. & STEFANOV, D. (1981): Rare alkalis in wall rock metasomatites of massive-pyrite deposits in central Srednogie, Bulgaria. *Geologica Balcanica* **11**(2), 89-102.
- CIOBANU, C.L., COOK, N.J. & STEIN, H. (2002): Regional setting and geochronology of the Late Cretaceous Banatitic Magmatic and Metallogenic Belt. *Mineral. Deposita* **37**, 541-567.
- CORBETT, G.J. & LEACH, T.M. (1998): Southwest Pacific Rim Gold–Copper Systems: Structure, Alteration, and Mineralization. *Soc. Econ. Geol., Spec. Publ.* **6**.

- DEEN, J.A., RYE, R.O., MUNOZ, J.L. & DREXLER, J.W. (1994): The magmatic hydrothermal system at Julcani, Peru: evidence from fluid inclusions and hydrogen and oxygen isotopes. *Econ. Geol.* **89**, 1924-1938.
- DIMITROV, C. (1960): Magmatismus und Erzbildung im Erzgebiet von Panagjuriste. *Freiberg Forschungshefte C* **79**, 67-81.
- DRIESNER, T. & HEINRICH, C.A. (2002): Revised critical curve for the system H₂O–NaCl. *Geochim. Cosmochim. Acta* **66**(15A), A196.
- EINAUDI, M.T. (1977): Environment of ore deposition at Cerro de Pasco, Peru. *Econ. Geol.* **72**, 893-924.
- FOURNIER, R.O. (1987): Conceptual models of brine evolution in magmatic-hydrothermal systems. In *Volcanism in Hawaii* (R.W. Decker, T.L. Wright & P.H. Stauffer, eds.), *U.S. Geol. Surv., Prof. Pap.* **1350**, 1487-1506.
- GOLDSTEIN, R.H. & REYNOLDS, T.J. (1994): Systematics of fluid inclusions in diagenetic minerals. *Soc. Sed. Geol., Short Course* **31**.
- HALL, A.J., CERVELLE, B. & LÉVY, C. (1974): The effect of substitution of Cu by Zn, Fe and Ag on optical properties of synthetic tetrahedrite, Cu₁₂Sb₄S₁₃. *Bull. Soc. fr. Minéral. Cristallogr.* **97**, 18-26.
- HANNINGTON, M.D., BLEEKER, W. & KJARSGAARD, I. (1999): Sulfide mineralogy, geochemistry, and ore genesis of the Kidd Creek deposit. II. The bornite zone. In *The Giant Kidd Creek Volcanogenic Massive Sulfide Deposit, Western Abitibi Subprovince, Canada* (M.D. Hannington & C.T. Barrie, eds.). *Econ. Geol., Monogr.* **10**, 225-266.
- HAYBA, D.O., BETHKE, P.M., HEALD, P. & FOLEY, N.K. (1985): Geologic, mineralogic, and geochemical characteristics of volcanic-hosted epithermal precious-metal deposits. In *Geology and Geochemistry of Epithermal Systems* (B.R. Berger & P.M. Bethke, eds.). *Rev. Econ. Geol.* **2**, 129-167.
- HEALD, P., FOLEY, N.K. & HAYBA, D.O. (1987): Comparative anatomy of volcanic-hosted epithermal deposits – acid-sulfate and adularia-sericite types. *Econ. Geol.* **82**, 1-26.
- HEDENQUIST, J.W., AOKI, M. & SHINOHARA, H. (1994): Flux of volatiles and ore-forming metals from the magmatic-hydrothermal system of Satsuma Iwojima volcano. *Geology* **22**, 585-588.
- _____, & ARRIBAS, A., JR. (1999): Epithermal gold deposits. I. Hydrothermal processes in intrusion-related systems. II. Characteristics, examples and origin of epithermal gold deposits. In *Epithermal Mineralization of the Western Carpathians* (F. Molnar, J. Lexa & J.W. Hedenquist, eds.). *Soc. Econ. Geol., Guidebook Ser.* **31**, 13-63.
- _____, & REYNOLDS, T.J. (1998): Evolution of an intrusion-centered hydrothermal system: Far Southeast – Lepanto porphyry and epithermal Cu–Au deposits, Philippines. *Econ. Geol.* **93**, 373-404.
- _____, ARRIBAS, R.A. & GONZALEZ-URIEN, E. (2000): Exploration for epithermal gold deposits. *Rev. Econ. Geol.* **13**, 245-277.
- _____, & LOWENSTERN, J.B. (1994): The role of magmas in the formation of hydrothermal ore deposits. *Nature* **370**(6490), 519-527.
- _____, & RICHARDS, J.P. (1998): The influence of geochemical techniques on the development of genetic models for porphyry copper deposits. In *Techniques in Hydrothermal Ore Deposits Geology* (J.P. Richards & P.B. Larson, eds.). *Rev. Econ. Geol.* **10**, 235-256.
- _____, SIMMONS, S.F., GIGGENBACH, W.F. & ELDRIDGE, C.S. (1993): White Island, New Zealand, volcanic-hydrothermal system represents the geochemical environment of high-sulfidation Cu and Au ore deposition. *Geology* **21**, 731-734.
- HEINRICH, C.A. (2003): Magmatic vapour condensation and the relation between porphyries and epithermal Cu–Au mineralisation: thermodynamic constraints. *Proc. 7th Biennial SGA Meeting (Athens)*.
- _____, GUNTHER, D., AUDETAT, A., ULRICH, T. & FRISCHKNECHT, R. (1999): Metal fractionation between magmatic brine and vapor, determined by microanalysis of fluid inclusions. *Geology* **27**, 755-758.
- JAMBOR, J.L. & OWENS, D.R. (1987): Vincienite in the Maggie porphyry copper deposit, British Columbia. *Can. Mineral.* **25**, 227-228.
- JANKOVIC, S. (1977): The copper deposits and geotectonic setting of Thethyan Eurasian metallogenic belt. *Mineral. Deposita* **12**, 37-47.
- KOUZMANOV, K. (2001): *Genèse des concentrations en métaux de base et précieux de Radka et Elshitsa (zone de Sredna Gora, Bulgarie): une approche par l'étude minéralogique, isotopique et des inclusions fluides*. Thèse de doctorat, Université d'Orléans, Orléans, France.
- _____, BAILLY, L., RAMBOZ, C., ROUER, O. & BÉNY, J.-M. (2002): Morphology, origin and infrared microthermometry of fluid inclusions in pyrite from the Radka epithermal copper deposit, Srednogorie zone, Bulgaria. *Mineral. Deposita* **37**, 599-613.
- _____, BÉNY, J.-M., RAMBOZ, C. & BAILLY, L. (2000a): CO₂–H₂, sericite- and kaolinite-bearing fluid inclusions from the Radka copper deposit, Sredna Gora zone, Bulgaria – evidence for advanced argillic alteration. *ABCD–GEODE 2000 Workshop (Borovets, Bulgaria), Abstr.*, 38.
- _____, BOGDANOV, K. & RAMBOZ, C. (2000b): Cu–Bi–Pb–Te mineral assemblage in the Elshitsa and Radka deposits, Sredna Gora zone, Bulgaria. *ABCD–GEODE 2000 Workshop (Borovets, Bulgaria), Abstr.*, 39.
- KOVALENKER, V.A. (1982): Tin minerals and their paragenesis in a subvolcanic gold deposit. *Geologiya Rudnykh Mestorozhdeniy* **24**(1), 31-41 (in Russ.).

- _____, EVSTIGNEVA, T.L., MALOV, V.S., TRUBKIN, N.B., GORSHKOV, A.I. & GEINKE, B.R. (1984): Nekrasovite $\text{Cu}_{26}\text{V}_2\text{Sn}_6\text{S}_{32}$ – new mineral from the colusite group. *Mineral. Zh.* **6**(2), 88-97.
- _____, TSONEV, D., BRESKOVSKA, V., MALOV, V.S. & TRONEVA, N.V. (1986): New data on the mineralogy of copper-pyrite deposits in the central Srednogorie zone, Bulgaria. In *Metasomatism, Mineralogy, and Genetical Features of Gold and Silver Deposits in Volcanic Areas* (D.S. Korjinsky, ed.). Nauka, Moscow, Russia, 91-110 (in Russ.).
- LEMIERE, B., DELFOUR, J., MOINE, B., PIBOULE, M., PLOQUIN, A., ISNARD, P. & TEGYEV, M. (1986): Hydrothermal alteration and the formation of aluminous haloes around sulfide deposits: a model for alterites at Chizeuil (Morvan, France). *Mineral. Deposita* **21**, 147-155.
- LOWENSTERN, J.B., MAHOOD, G.A., RIVERS, M.L. & SUTTON, S.R. (1991): Evidence for extreme partitioning of copper into a magmatic vapor phase. *Science* **252**(5011), 1405-1409.
- LÜDERS, V. (1996): Contribution of infrared microscopy to fluid inclusion studies in some opaque minerals (wolframite, stibnite, bournonite): metallogenic implications. *Econ. Geol.* **91**, 1462-1468.
- _____. (1999): Infrared microscopy applied to studies of mineral-hosted fluid inclusions. *Hamamatsu Euro News* **2**, 19.
- MANCANO, D.P. & CAMPBELL, A.R. (1995): Microthermometry of enargite-hosted fluid inclusions from the Lepanto, Philippines, high-sulfidation Cu–Au deposit. *Geochim. Cosmochim. Acta* **59**, 3909-3916.
- MARCOUX, E., MOËLO, Y. & MILÉSI, J.P. (1994): Vinciennite and Cu-excess tennantite from the Layo (Cu, Sn, As, Au) epithermal deposit (southern Peru). *Mineral. Petrol.* **51**, 21-36.
- MASKE, S. & SKINNER, B.J. (1971): Studies of the sulfosalts of copper. 1. Phases and phase relations in the system Cu–As–S. *Econ. Geol.* **66**, 901-918.
- MILEV, V.R., STANEV, V.B. & IVANOV, V.H. (1996): Statistical manual of the ore production in Bulgaria during 1878–1995. Zemia 99 Publishing House, Sofia, Bulgaria (in Bulg.).
- MORITZ, R., PETRUNOV, R., JACQUAT, S. & CHAMBEFORT, I. (2002): Microthermometry of enargite from the Upper Cretaceous high-sulfidation Au–Cu Chelopech deposit, Bulgaria. In *Program with Abstracts, PACROFI VIII* (D.J. Kontak & A.J. Anderson, eds.), 73-74.
- MUNTEAN, J.L. & EINAUDI, M.T. (2001): Porphyry–epithermal transition: Maricunga belt, northern Chile. *Econ. Geol.* **96**, 743-772.
- MUROWCHICK, J.B. & BARNES, H.L. (1986): Marcasite precipitation from hydrothermal solutions. *Geochim. Cosmochim. Acta* **50**, 2615-2629.
- PETRUNOV, R. (1994): *Mineral Parageneses and Physico-chemical Conditions of Ore Formation in the Chelopech Deposit*. Ph.D. thesis, Geological Institute, Bulgarian Academy of Sciences, Sofia, Bulgaria (in Bulg.).
- _____, DRAGOV, P. & NEYKOV, H. (1991): Polyelemental (with As, Sn, V, Bi, Ag, Te, Ge, Se, etc.) mineralizations in the Asarel porphyry copper deposit. *Rev. Bulg. Geol. Soc.* **52** (1), 1-8 (in Bulg.).
- POPOV, P. (1996): Characteristic features of the Banat–Srednogorie metallogenic belt. In *Plate Tectonic Aspects of the Alpine Metallogeny in the Carpatho-Balkan Region* (P. Popov, ed.). *UNESCO IGCP Project 356, Proc. Annual Meeting* **1**, 137-154.
- _____ & POPOV, K. (1997): Metallogeny of Panagyurishte ore region. In *Symp. on Ore Deposits Exploration* (K. Romić & R. Kondzulović, eds.). Belgrade, 327-338.
- POSFAL, M. & BUSECK, P.R. (1998): Relationships between microstructure and composition in enargite and luzonite. *Am. Mineral.* **83**, 373-382.
- POUCHOU, J.L. & PICHOR, F. (1984): Un nouveau modèle de calcul pour la microanalyse quantitative par spectrométrie de rayons X. I. Application à l'analyse d'échantillons homogènes. *La Recherche Aérospatiale* **3**, 167-192.
- RADONOVA, T. (1962): Primary mineralization and wall-rock alterations in the area of Radka mine, in the vicinity of Panagyurishte. *Travaux sur la Géologie de Bulgarie, Série "Géochimie, Gîtes métallifères et non-métallifères"* **3**, 93-128 (in Bulg.).
- ROEDDER, E. (1984): Fluid Inclusions. *Rev. Mineral.* **12**.
- SAWKINS, F.J. (1964): Lead–zinc ore deposition in the light of fluid inclusion studies, Providencia mine, Zacatecas, Mexico. *Econ. Geol.* **59**, 883-919.
- SHINOHARA, H. & HEDENQUIST, J.W. (1997): Constraints on magma degassing beneath the Far Southeast porphyry Cu–Au deposit, Philippines. *J. Petrol.* **38**, 1741-1752.
- SILLITOE, R.H. (1985): Ore-related breccias in volcanoplutonic arcs. *Econ. Geol.* **80**, 1467-1514.
- _____. (1999): Styles of high-sulfidation gold, silver and copper mineralization in porphyry and epithermal environments. In *PacRim '99, Proc. Austral. Inst. Mining Metall.* (Bali), 29-44.
- _____, HALLS, C. & GRANT, J.N. (1975): Porphyry tin deposits in Bolivia. *Econ. Geol.* **70**, 913-927.
- SIMMONS, S.F. & BROWNE, P.R.L. (1997): Saline fluid inclusions in sphalerite from the Broadlands–Ohaaki geothermal system: a coincidental trapping of fluids being boiled toward dryness. *Econ. Geol.* **92**, 485-489.
- SOURIRAJAN, S. & KENNEDY, G.C. (1962): System H_2O – NaCl at elevated temperatures and pressures. *Am. J. Sci.* **260**, 115-141.

- SPRY, P.G., MERLINO, S., WANG, S., ZHANG, X.M. & BUSECK, P.R. (1994): New occurrences and refined crystal chemistry of colusite, with comparisons to arsenosulvanite. *Am. Mineral.* **79**, 750-762.
- STANISHEVA-VASSILEVA, G. (1980): The Upper Cretaceous magmatism in Srednogorie zone, Bulgaria: a classification attempt and some implications. *Geologica Balcanica* **10**(2), 15-36.
- STERNER, S.M., HALL, D.L. & BODNAR, R.J. (1988): Synthetic fluid inclusions. 4. Solubility relations in the system NaCl-KCl-H₂O under vapor-saturated conditions. *Geochim. Cosmochim. Acta* **52**, 989-1005.
- STRASHIMIROV, S. (1982): Sulvanite and colusite from the Medet molybdenum-copper deposit. *Geochemistry, Mineralogy and Petrology, Sofia* **15**, 57-66 (in Bulg.).
- _____ & KOVACHEV, V. (1992): Temperatures of ore formation in copper deposits from the Srednogorie zone based on fluid inclusion studies of minerals. *Rev. Bulg. Geol. Soc.* **53**, 1-12 (in Bulg.).
- _____, PETRUNOV, R. & KANAZIRSKI, M. (2002): Porphyry-copper mineralisation in the central Srednogorie zone, Bulgaria. *Mineral. Deposita* **37**, 587-598.
- TERZIEV, G. (1966): Kostovite, a gold-copper telluride from Bulgaria. *Am. Mineral.* **51**, 29-36.
- THOUVENIN, J.M. (1983): *Les minéralisations polymétalliques à Pb-Zn-Cu-Ag de Huaron (Pérou central)*. Thèse de doctorat, Ecole Normale Supérieure des Mines, Paris, France.
- TSONEV, D., BOGDANOV, K. & POPOV, K. (2000a): The volcanic-hosted sulphide (VHS) deposits from the southern part of the Panagyurishte ore region, Bulgaria. *ABCD-GEODE 2000 Workshop, (Borovets, Bulgaria), Abstr.*, 85.
- _____, POPOV, K., KANAZIRSKI, M. & STRASHIMIROV, S. (2000b): Radka ore field. In *Geology and Metallogeny of the Panagyurishte Ore Region, Srednogorie Zone, Bulgaria* (S. Strashimirov & P. Popov, eds.). *ABCD-GEODE 2000 Workshop, Guide to Excursions (A and C)*, 32-39.
- TZONEV, D. (1982): Radka copper-pyrite-polymetallic deposit. In *Guidebook 2: Central Srednogorie* (L. Vassileff, D. Tzonev & I. Bonev, eds.). *Int. Mineral. Assoc., 13th Gen. Meeting (Varna)*, 23-36.
- VON QUADT, A., IVANOV, Z. & PEYCHEVA, I. (2001): The Central Srednogorie (Bulgaria) part of the Cu (Au-Mo) belt of Europe: a review of the geochronological data and the geodynamical models in the light of the new structural and isotopic studies. In *Mineral Deposits at the Beginning of the 21st Century* (A. Piestrzynski *et al.*, eds.). *Proc. Joint Sixth Biennial SGA-SEG Meeting (Krakow)*, 555-558.
- WHITE, N.C. & HEDENQUIST, J.W. (1990): Epithermal environments and styles of mineralization: variations and their causes, and guidelines for exploration. *J. Geochem. Explor.* **36**, 445-474.
- WILLIAMS-JONES, A.E., MIGDISOV, A.A., ARCHIBALD, S.M. & XIAO, Z. (2002): Vapor-transport of ore metals. In *Water-Rock Interactions, Ore Deposits, and Environmental Geochemistry* (R. Hellmann & S.A. Wood, eds.). *Geochem. Soc., Spec. Publ.* **7**, 279-305.

Received December 5, 2002, revised manuscript accepted June 13, 2003.